PB83-204164

FINAL REPORT

PRESSURES ON COASTAL BRIDGES DUE TO NORMAL INCIDENCE WAVES

MSHD-RD-81-076

by

Keith Denson

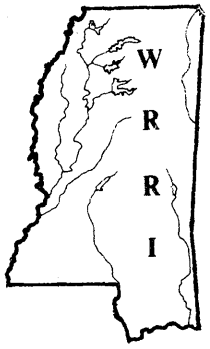

Conducted by
Mississippi Water Resources Research Institute
and
Department of Civil Engineering
Mississippi State University
for
Mississippi State Highway Department
in cooperation with the
U.S. Department of Transportation
Federal Highway Administration

1981

Technical Report Documentation Page

1. Report No.	2. Government Accession No.	3. Recipient's Catalog No.
FHWA-MSHD-RD-81-076		PB83 204164

4. Title and Subtitle	5. Report Date
Pressures on Coastal Bridges Due To Normal Incidence Waves	December 1981
	6. Performing Organization Code
7. Author(s) Keith H. Denson	8. Performing Organization Report No. MSHD-RD-81-076
9. Performing Organization Name and Address Water Resources Research Institute Mississippi State University	10. Work Unit No. (TRAIS) 11. Contract or Grant No.
12. Sponsoring Agency Name and Address Mississippi State Highway Department	13. Type of Report and Period Covered Final Report Oct. 1, 1980-Sept. 30, 1981
	14. Sponsoring Agency Code S01274

15. Supplementary Notes

Prepared in cooperation with the U.S. Department of Transportation, Federal Highway Administration

16. Abstract

Local pressures due to water waves were measured at discrete points along the underside of two 1:24 scale model bridges for various water depths and wave heights. One model was of a four-lane slab and beam bridge carrying traffic along two structurally separated lane pairs supported by a common pile bent. The other model was of a trapezoidal box girder bridge with superelevation to seaward. The slab/beam model was geometrically similar to the Bay St. Louis, Mississippi, bridge which was heavily damaged by Hurricane Camille in 1969. The second model was of a proposed interstate connector at Biloxi, Mississippi. Results of the research are presented in dimensionless form for use on geometrically similar bridges.

17. Key Words	18. Distribution Statement
Bridges, Waves, Pressures, Physical Modeling, Hurricanes	Unlimited

19. Security Classif. (of this report)	20. Security Classif. (of this page)	21. No. of Pages	22. Price
Unclassified	Unclassified	90	

Form DOT F 1700.7 (8-72) Reproduction of completed page authorized

FINAL REPORT

PRESSURES ON COASTAL BRIDGES DUE TO NORMAL INCIDENCE WAVES

by

Keith H. Denson
Professor
Department of Civil Engineering
Mississippi State University

Water Resources Research Institute
Mississipi State University
Mississippi State, MS 39762

PREFACE

The work upon which this report is based was supported by the Mississippi State Highway Department in cooperation with the Federal Highway Administration. This support is gratefully acknowledged.

The author would like to thank Mr. Bennie D. Verell, Bridge Engineer, Mr. T. C. Teng, former Research and Development Engineer, and Mr. Joe P. Sheffield, Research and Development Engineer of the Mississippi State Highway Department for their cooperation and assistance.

Mohammad Jahadi served as the primary research assistant on this project and was assisted by several undergraduates in the Department of Civil Engineering, Mississippi State University.

NOTATION

c: wave celerity

g: acceleration of gravity

h: height of bridge slab above mud line

p: local pressure due to wave action

x: location of pressure measurements

D: still water depth

G: specific weight of water, replacing the standard symbol, γ , for computer plotting

H: wave height, trough to crest

H_0: actual overwash height of a wave above top of slab

H_T: theoretical overwash height of a wave above top of slab

W: outside-to-outside width of a pair of bridge lanes; used as the significant reference geometric variable

SUMMARY

This research experimentally determined local pressures at discrete points on the underside of two 1:24 scale bridge models due to normal incidence waves. The first model was of the Bay St. Louis, Mississippi, bridge on U.S. Highway 90 which was severely damaged by Hurricane Camille in 1969. This model is of a slab/beam bridge, four-lane, with the two lane pairs structurally separated and supported on a common pile bent. The second bridge model was of a trapezoidal box girder with superelevation to seaward, proposed as a connector on I-110 near Biloxi, Mississippi.

In both models, pressures were measured at midspan and near the supports. Five pressure points were located at each section on the slab/beam model and six were located at each section on the box girder. Pressures were measured with a one-half inch diameter electrical transducer which was connected to an oscillograph. Pressures were measured for both the seaward and landward lane pairs for five water depths and five wave heights. 500 bits of data were recorded for the slab/beam model and 600 for the box girder. Results are displayed in dimensionless form for conversion to prototype quantities.

In addition to the primary pressure measurements, wave overwash was evaluated for the seaward lanes of the slab/beam bridge. The depth of overwash was found to be expressible as a two variable

linear function of theoretical overwash and bridge height to water depth ratio.

The results of this research should be of value to bridge designers in predicting the capacity of local bridge structural elements for withstanding pressures due to extreme waves.

Table of Contents

List of Figures

List of Tables

PRESSURES ON COASTAL BRIDGES DUE TO NORMAL INCIDENCE WAVES

CHAPTER I

INTRODUCTION

Coastal bridges can be exposed to heavy damage during hurricane conditions. The most severe damage is caused by a general rise in water surface elevation, often called a "hurricane surge" or a "tide", and the accompanying extreme winds which generate surface waves. The combination of these two effects often places bridge superstructures, which are normally well above the water surface, within reach of surface waves. The forces and pressures produced by these waves have not been available to bridge designers in the past. The bridge engineers of 21 coastal states were surveyed by the author in the fall of 1978 and not a single state of the 19 replying had a design policy based on known wave forces and pressures. Six of the states replying had bridges previously damaged by hurricane waves and sixteen had bridges which could be exposed to hurricane wave action. Since the time of the questionnaire, two additional states have had coastal bridges completely destroyed by wave action. One of these bridges was the Dauphin Island (Alabama) causeway which was destroyed by Hurricane Frederic in 1979. This bridge was a two-lane concrete bridge supported on pile bents. A television report of a helicopter fly-over after the hurricane, seen by the author, indicated that the entire superstructure of the causeway had been swept from the pile bents.

In 1969, Hurricane Camille struck the Mississippi Gulf Coast and severely damaged the Bay St. Louis and the Biloxi Bay bridges. These bridges were not destroyed but suffered a displacement of some spans which resulted in an expensive rehabilitation project. These bridges appeared to have experienced a loss of positive vertical reaction on the supporting pile bents and a subsequent horizontal transport of some spans.

With information obtained from a literature review indicating that no previous work had been done to quantitatively measure wave forces on bridge models Denson (1) in the summer of 1978 conducted a two-dimensional study of wave forces and moments on a 1:24 model of the Bay St. Louis bridge cross-section. The results of that study indicated the feasibility of determining these quantities for coastal bridges and the predictability of damage of the type experienced by the Bay St. Louis bridge under certain combinations of water depth and wave height.

With the results of the 1978 study available, a two-year project was begun in the fall of 1978 to study the six total wave forces and moments acting on two different bridge models for various angles of wave incidence. This study was funded by the Mississippi State Highway Department and the Federal Highway Administration. The results of this project were presented in a final report (2) to the Mississippi State Highway Department in August 1981, and the results again demonstrated the severe forces which could result from hurricane-generated waves.

In addition to total force and moment resultants caused by wave action which can only be used to estimate superstructure to foundation reactions and overall stability and foundation requirements, bridge designers are in need of some quantitative estimate of local pressures which may act on elements of the bridge superstructure. This information would be of use in the design of slab and beam elements of bridge superstructures.

The present project was begun to determine the magnitude of local pressures at discrete points on the two bridge models used in the total force and moment project (2). The first of the models tested was a 1:24 scale model of the Bay St. Louis, Mississippi, bridge on U.S. Highway 90. This bridge is a four-lane slab and beam type bridge with the two pairs of lanes structurally separated but supported on a common pile bent. The second model was a 1:24 scale model of a trapezoidal box girder with superelevation to seaward. This bridge is a part of a proposed I-110 connector at Biloxi, Mississippi.

Objective. The objective of this research was to measure local pressures at discrete points along the underside of both models along the center of a span and near the end supports of the spans for normal incidence waves only. Normal incidence waves were chosen because the previous work by Denson (2) indicated that normal incidence waves were most likely to create the most severe overall effects on bridge structures. Bridge heights were to be

at a fixed elevation above the mud line while water depth and wave height were to be varied. Results were to be presented in dimensionless form for scaling to prototype quantities.

CHAPTER II

METHODS AND PROCEDURES

Wave Generation. The three-dimensional wave basin at Mississippi State University was utilized in this study. The basin is 40 feet long and the active test section for this study was 16 feet wide. A coarse gravel beach is installed along the end of the wave basin as a wave energy absorber to minimize reflection. The maximum water depth used in the study was 13 inches which corresponded to 26 feet on the 1:24 scale models.

Waves were generated at a constant period of 3 seconds on the models. The shape of the waves generated was generally trochoidal in form with a relatively long trough and a much shorter crest. Total wave height was divided in the approximate ratios of two-thirds for the crest height above still water elevation and one-third for the trough depression below still water level. Such waves as those generated for this research are termed "shallow water waves" and wave length and period are relatively insignificant. Wave celerity is uniquely determined by water depth and the acceleration of gravity while wave forces are highly dependent on wave height and water depth.

The wave generator used in the study is of a horizontal piston type and is capable of generating waves up past the point of breaking. Wave forces reach a maximum at the point of incipient breaking and diminish thereafter. The largest wave height to depth ratio which could be generated without breaking was approximately 0.5.

Model Construction. Both of the models used in this research were constructed to a scale of 1:24. The models had previously been utilized in the total force and moment project (2). The slab/beam bridge model was a true hydraulic model of the Bay St. Louis bridge except for a slight taper to the underside of the walkway along the exterior edges of the bridge and the absence of an open guard rail along those edges. The Bay St. Louis bridge is a slab and beam bridge constructed of reinforced concrete. The seaward and landward pairs of lanes are supported on a common reinforced concrete pile bent. Figure 2.1 shows the proportions of the cross-section of a single pair of lanes related to the width of the bridge while Figure 2.2 shows the geometric relation between the pile bent, bridge height and span length to the width. The reference width, W, on the slab/beam model was 15.73 inches, corresponding to 3.146 feet in the prototype. The height relationship shown is a compromise with the actual bridge which has ascending and descending portions leading up to and away from a movable central section. The height chosen represents a distance of 22 feet on the prototype from the mud line to the top of the slab. The slab/beam model was constructed principally of wood with a plexiglass central span utilized for data acquisition. The test section was drilled and tapped at 5 points along the center line of the span and at 5 points near the end of the span to receive a pressure transducer housing or plugs which were used to block the holes not occupied by the transducer. These locations were centered on the two overhangs and midway between beams and are indicated in Figure 2.2.

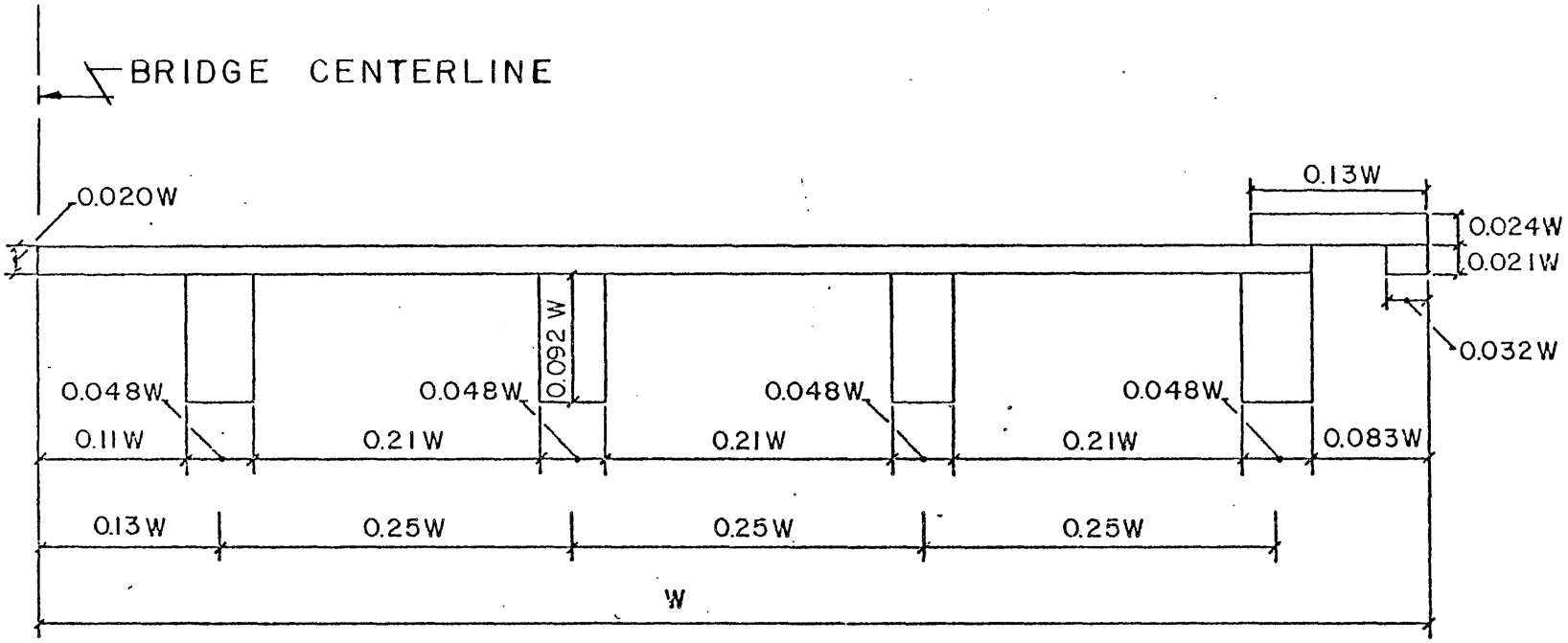

BRIDGE CROSS-SECTION (2 LANES)

Figure 2.1 Cross-Section of Slab/Beam Bridge Model

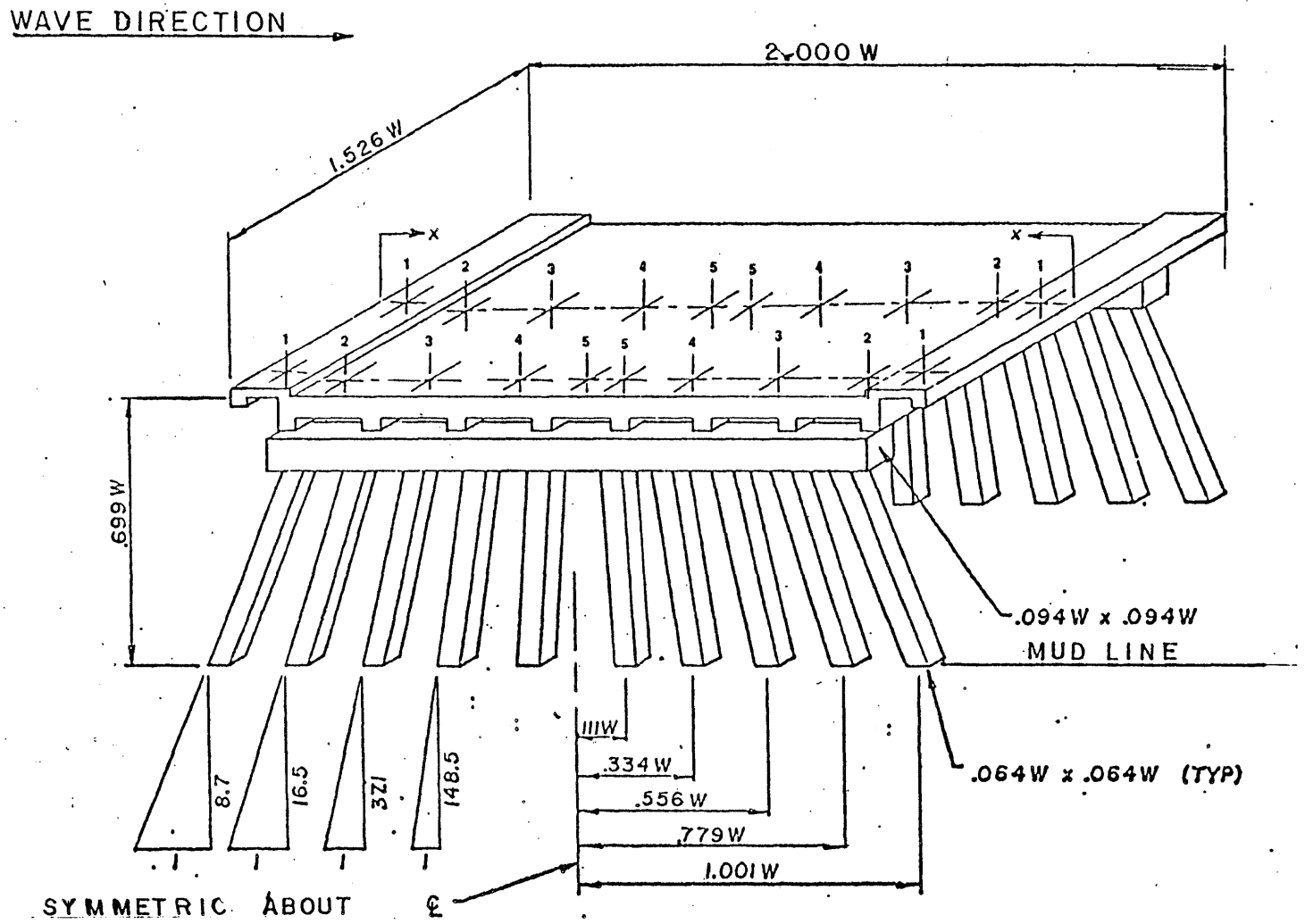

Figure 2.2 Isometric of Slab/Beam Bridge Model with Pressure Transducer Locations

The second model utilized in this study was a 1:24 scale model of a proposed connector route at Biloxi, Mississippi. The proposed structure is a trapezoidal box girder and has superelevation to seaward because of a curved prototype alignment. The curved alignment was not modeled, but a straight section considered representative of the most seaward section was. Superelevation of 0.10 feet/foot was included in the test span. The cross-section of this model is shown in Figure 2.3 which relates the proportions of the model to the horizontal width of a pair of lanes. The pairs of lanes making up the four-lane connector are separated by a horizontal distance of 45 feet, center-to-center. The reference length W on the model was 13.4 inches corresponding to 26.8 feet on the prototype. The model was constructed of laminated wood sections which were planed to dimension. The test section was also wood with a metal ring set flush with the under surface to receive a threaded pressure transducer housing inserted from the top. The transducer locations were at both overhangs, one point on each of the beveled sides and at two points across the bottom for a total of six. Transducer location lines were at mid-span and near one of the piers. The locations are indicated on Figure 2.3.

Instrumentation. Wave heights were pre-recorded for various water depths used in the study versus the indexed setting of an eccentric crank on the wave generator. Wave heights were recorded at the model locations before the models were installed because of the

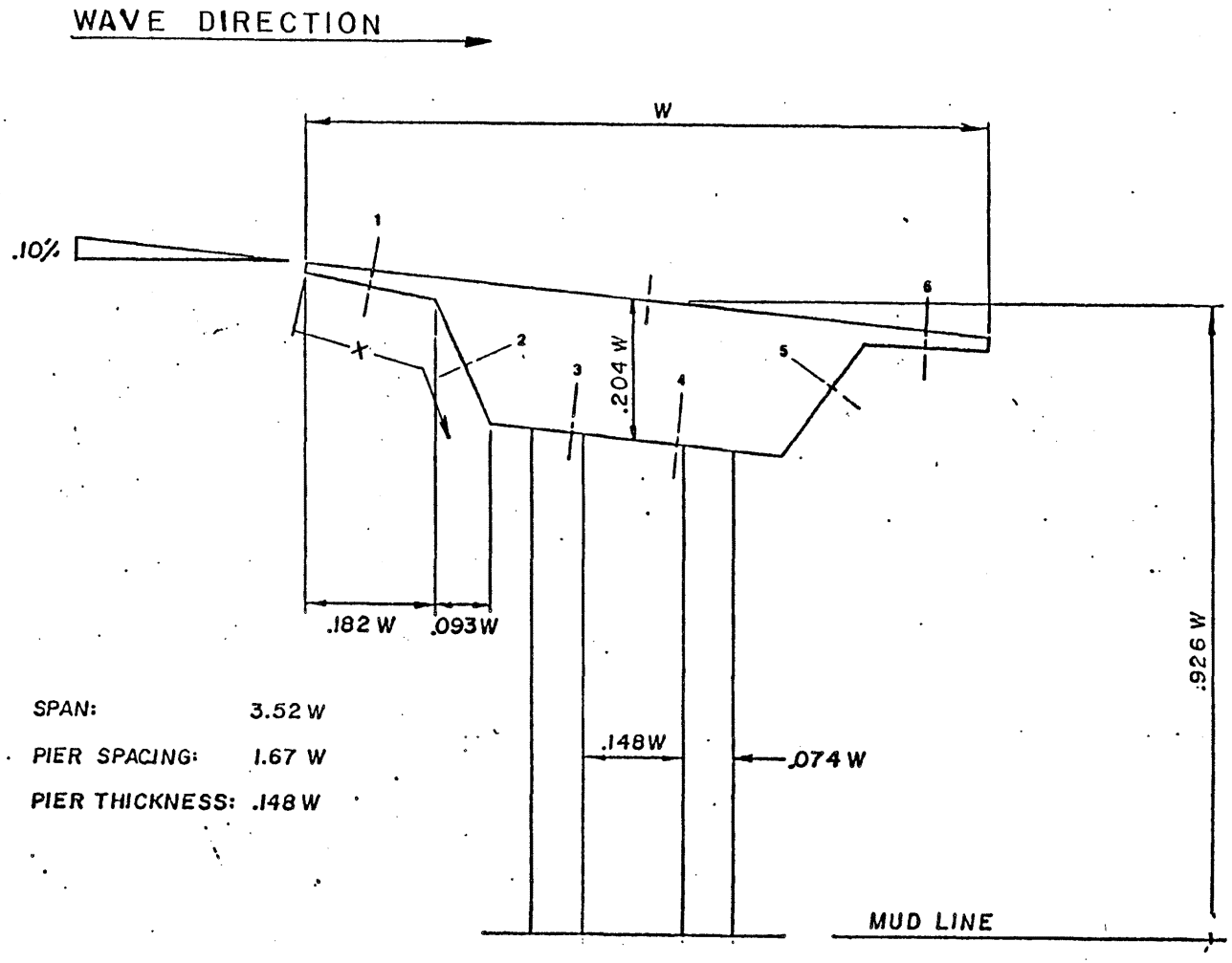

Figure 2.3 Box Girder Bridge Model with Pressure Transducer Locations

extreme turbulence generated by impacting waves. The wave heights would, thus, represent more nearly a wave approaching from seaward before its behavior was appreciably influenced by the presence of the model. Figure 2.4 is a schematic of the circuitry utilized for the wave probe and was used in a half-bridge circuit connected to a carrier amplifier oscillographic recorder. The same circuit as shown in Figure 2.4 was also used as a wave strike indicator installed along the leading edge of the more seaward pair of lanes. The probe of Figure 2.4 was replaced in this case with a pair of thin, bare copper wires cemented to the leading edge of both models.

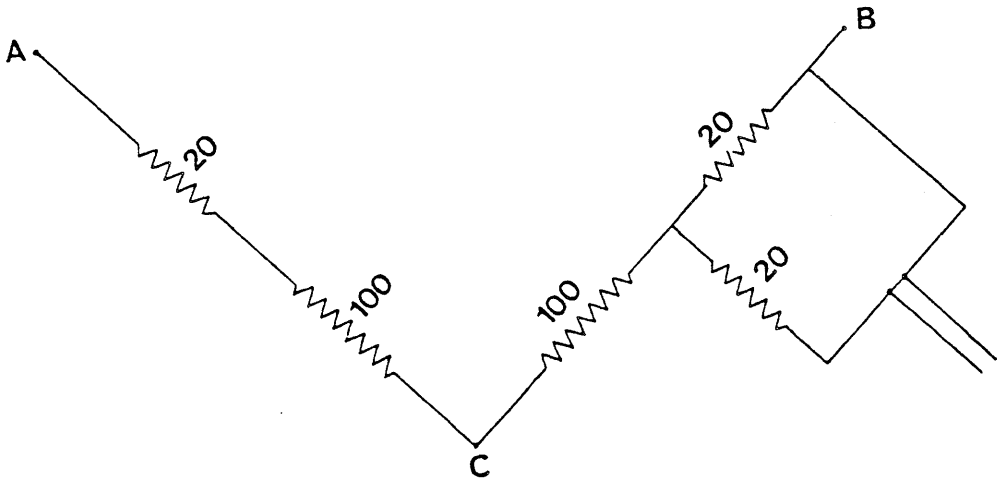

Figure 2.4 Schematic of Wave Probe Circuitry

Pressures were measured along the underside of both models at the locations shown in Figures 2.1 and 2.3. The pressure transducer used was a Statham, 1/2 inch diameter, 0 $\pm$ 5 psig, flush diaphragm instrument. The same transducer was used at each of the locations shown in Figures 2.2 and 2.3 along the mid-span line of each model and near the supports. Pressures were measured for both the seaward and landward lane pairs of both bridges. The pressure transducer was calibrated prior to initial use and several times during the test program with a hydrostatic test stand. During testing, the pressure transducer was connected in a full-bridge circuit to a Sanborn two-channel carrier amplifier oscillographic recorder at a remote location. One channel of the recorder was utilized for the transducer signal while the other was used for the signal from the wave strike indicator. Figure 2.5 illustrates a typical data trace from the pressure transducer.

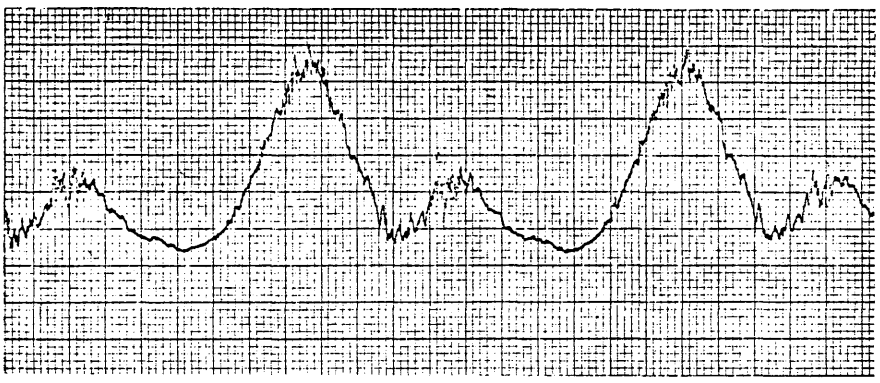

Figure 2.5 Typical Data Trace

Dimensional Considerations. The dependent variable resulting from this study was gage pressure (p) measured on the underneath surface of both bridges. The significant independent variables were width of a two-lane bridge structural section (W), gage locations (x), height of the bridge above the mud-line (h), still water depth (D), wave height (H), and specific weight of water (G). The standard variable (γ) for specific weight was not used because of the non-availability of the symbol in the computer plotting library available.

For the shallow water, long waves, generated for this study, wave length and wave period do not appreciably affect pressures generated by the waves. The wave celerity is highly significant for these problems but is uniquely determined with sufficient accuracy by the expression $c = \sqrt{g\ D}$; thus, celerity is not independent of water depth (D). Wave lengths used during these tests varied from 14.7 feet for a depth of 9 inches to 17.7 feet at a depth of 13 inches. These wave lengths for the prototype are 354 feet and 425 feet, respectively. Wave period was held constant in the model tests at 3 seconds and corresponds to a period of 14.7 seconds for the prototype.

A dimensional matrix of the variables used in this study is shown in Table 2.1.

Table 2.1

Dimensional Matrix of Variables

Variable	Force	Length
p	1	-2
W	0	1
x	0	1
D	0	1
H	0	1
G	1	-3
*h	0	1

*A constant relation to W for each bridge; shown in Figures 2.2 and 2.3.

Including the variable h which forms a constant ratio with W for each bridge, the variables may be expressed in dimensionless functional form as:

$$p/GH = f\left(\frac{H}{D}, \frac{h}{D}, \frac{x}{W}, \frac{h}{W}^{**}\right)$$

**A constant for each bridge

There are many ways of correctly combining the variables in dimensionless form. Those chosen were considered logical for the independent variables while the choice of the dependent variable, p/GH, was made in an effort to normalize the pressure with respect to wave height in order to possibly obtain a more general relationship than might otherwise ensue. The results of this choice were to a large extent successful.

Test Procedures. The test procedure for each bridge consisted of installing the model in the wave basin at a 90 degree wave incidence angle with the active test section to seaward and the pressure transducer installed in one of the test ports. The transducer housing was inserted into a threaded circular hole at one of the locations shown in Figure 2.2 or 2.3. Care was taken to insure that the transducer diaphragm was flush with the underneath surface of the model during installation. At other pressure locations, flush-mounted plugs were installed to prevent disruption of the general flow pattern under the models. The water depth was initialized at 9 inches for the slab/beam model (18 feet prototype) and the wave generator was set to produce an H/D ratio of approximately 0.2. The wave machine was started and the wave allowed to stabilize before beginning a data trace. The stabilization required approximately 30 seconds during which 10 waves would have formed. A data trace

was obtained by starting the oscillographic recorder and observing a minimum of 5 waves to insure proper functioning of the instrumentation and to observe the periodicity of the data. After obtaining a data trace for one location the wave generator was stopped while the transducer was moved to another location of the ten on the slab/beam bridge and a plug was inserted into the previous test port. The wave generator was again started and another data trace obtained. After pressures at all ten locations on the seaward lanes had been read, the H/D ratio was varied to a larger value and the process repeated. A total of five H/D ratios were used up to the point of incipient wave breaking. After five values of H/D, the water depth was incremented by one inch (2 feet prototype) and the process repeated. A total of five water depths were used up through 13 inches (26 feet prototype) for the slab/beam model.

When the testing was completed on the seaward pair of lanes, the entire process was repeated for the landward pair of lanes. At the completion of the test series for the slab/beam bridge 500 individual pressure data traces were available.

The process described for the slab/beam bridge was duplicated in the test program for the box girder. The box girder model had six pressure transducer locations at the mid-span line and six near the pier supports. The box girder bridge reference height was somewhat above that of the slab/beam from the mud line and the water

depths were varied from 9 inches to 13 inches in one inch increments. These distances correspond to the depths of 18 feet to 26 feet on the prototype in two foot increments. A total of 600 data traces were taken from the box girder model including seaward and landward lanes.

CHAPTER III

RESULTS

Data Reduction. The raw data from the oscillograph recorder contained the basic data trace while the operator had recorded by hand on the data trace the water depth, the wave height to depth ratio, the location of the transducer on the model, seaward or landward lanes, box girder or slab/beam model and the attenuation factor used to record the pressure. After the data were examined by the principal investigator, it was decided that the time lag between peak pressures at different locations across the bridge was so short as to be practically indiscernible. The decision was made to display the reduced data in terms of peak positive and negative pressures at each location. Positive pressure was defined in the usual sense as being directed inward toward the surface of the model and negative pressure represented a suction on the surface.

A computer plotting program was written to non-dimensionalize the raw data, to plot points of peak pressures versus position on the model and to interconnect the plotted points with straight line segments for clarity in reading. No attempt was made to fit a continuous curve to the data since the pressure variation was most likely not a smooth function, particularly for the slab/beam bridge.

The print-out of the computer plotting program is reproduced in Appendix A and the dimensionless results are given for the slab/beam bridge and the box girder bridge in Appendices B and C, respectively.

The selection of the independent variable as p/GH tended to normalize the p/GH values relative to the independent variable H/D. This indicates that to a large extent, pressure is a linear function of wave height. While this relation is not true in all cases, the tendency is dominant in both bridge models. The author considers this to be a significant result.

Wave overwash characteristics were evaluated for the seaward lanes of the box girder bridge during the latter stages of this project. This information is needed to effectively design the slab and beam elements of the bridge since the hydrostatic pressure contributes to the total slab load along with pressures produced on the bottom surface of the slab.

The wave overwash characteristics were evaluated by measuring the maximum depth of water at the leading edge of the slab/beam seaward lanes and developing a unique equation for determining the water depth across the top of the bridge slab for various still water depths and wave heights. An undisturbed wave form of the type generated for this research has a total wave height, trough to crest, divided such that 2/3 of the wave height consists of crest

elevation above still water and 1/3 consists of trough depression below still water. The theoretical elevation of the crest of an undisturbed wave approaching the bridge above the top of the slab can be calculated as:

$$H_T = \left(\frac{2}{3} H + D \right) - h \qquad 3\text{-}1$$

where H_T is the theoretical water depth above the top of the slab, h is the top of slab elevation above the mud line, H is total wave height and D is still water depth. Because of reflection from the bridge, the wave form is altered from its undisturbed state and the water depth over the bridge is also increased because of crest particle velocities exceeding what corresponds to critical channel flow. Measurements of actual water depth, H_0, were taken over a range of twelve combinations of water depth and wave height and fit the planar equation:

$$H_0/h = 1.19\ H_T/h + 0.829\ h/D - 0.754 \qquad 3\text{-}2$$

Values of H_0 can be obtained for negative values of H_T because of altered wave forms and the fact that some overwash occurs when the wave crest strikes the beam on the seaward side of the bridge.

The data from which equation 3-2 is obtained are shown in Figure 3.1.

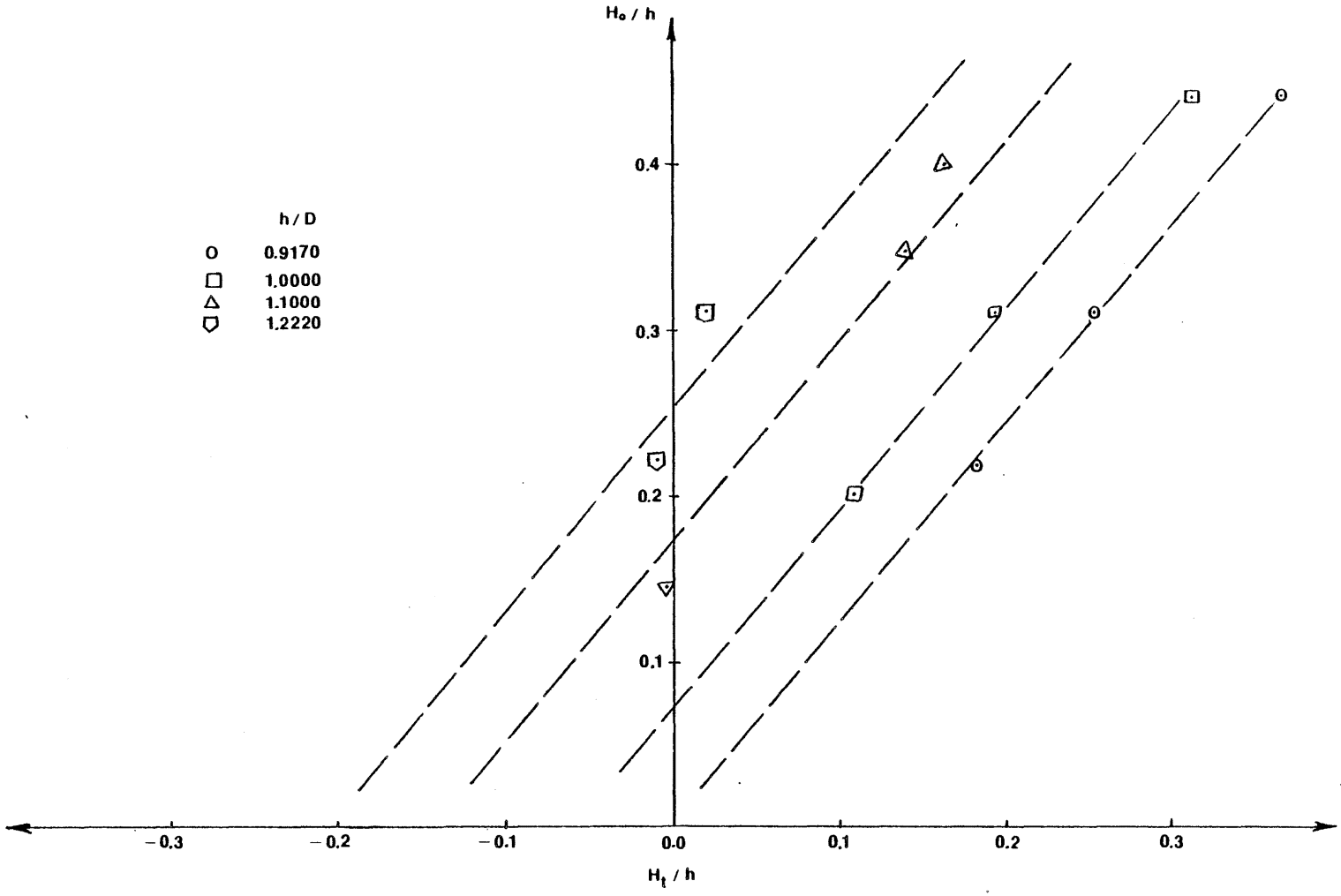

Figure 3.1 Wave Overwash Characteristics for Slab/Beam Bridge Seaward Lanes

Example on the Use of Design Curves. Figures 3.2 and 3.3 are duplicates of two of the design curves from Appendix B.

Given Data. A slab/beam bridge geometrically similar, in all respects, to the Bay St. Louis bridge.

Height of slab above bay bottom = 22 feet

Estimated hurricane surge water depth = 22 feet

Anticipated wave height = 8.8 feet.

Calculate:

$h/D = 22/22 = 1.00$

$H/D = 8.8/22 = 0.4$

Enter Figure 3.3 for pressures along the midspan line seaward lanes.

The peak positive pressures are nearly constant along the bridge and are

$+ p/GH = 1.00$

$- p/GH = 0.20$

The prototype values of p are, for an 8.8 foot wave:

$+ p = 1.00 \times 64.0 \times 8.8 = + 563$ PSF

$- p = 0.20 \times 64.0 \times 8.8 = - 113$ PSF

Near the ends of the span, enter Figure 3.2:

$+ p/GH = 1.00$

$- p/GH = 0.20$

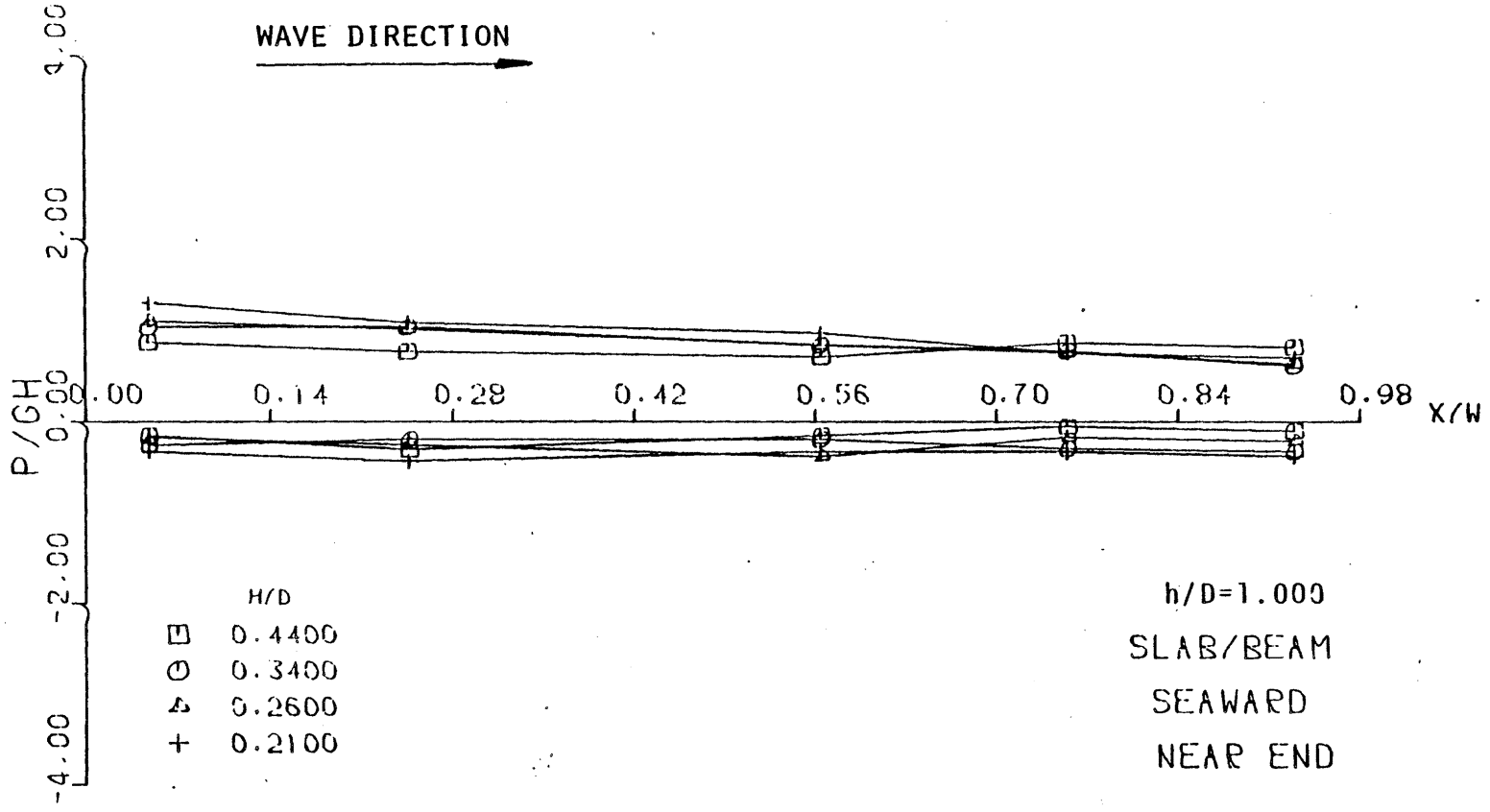

Figure 3.2 Design Curve for Slab/Beam Bridge

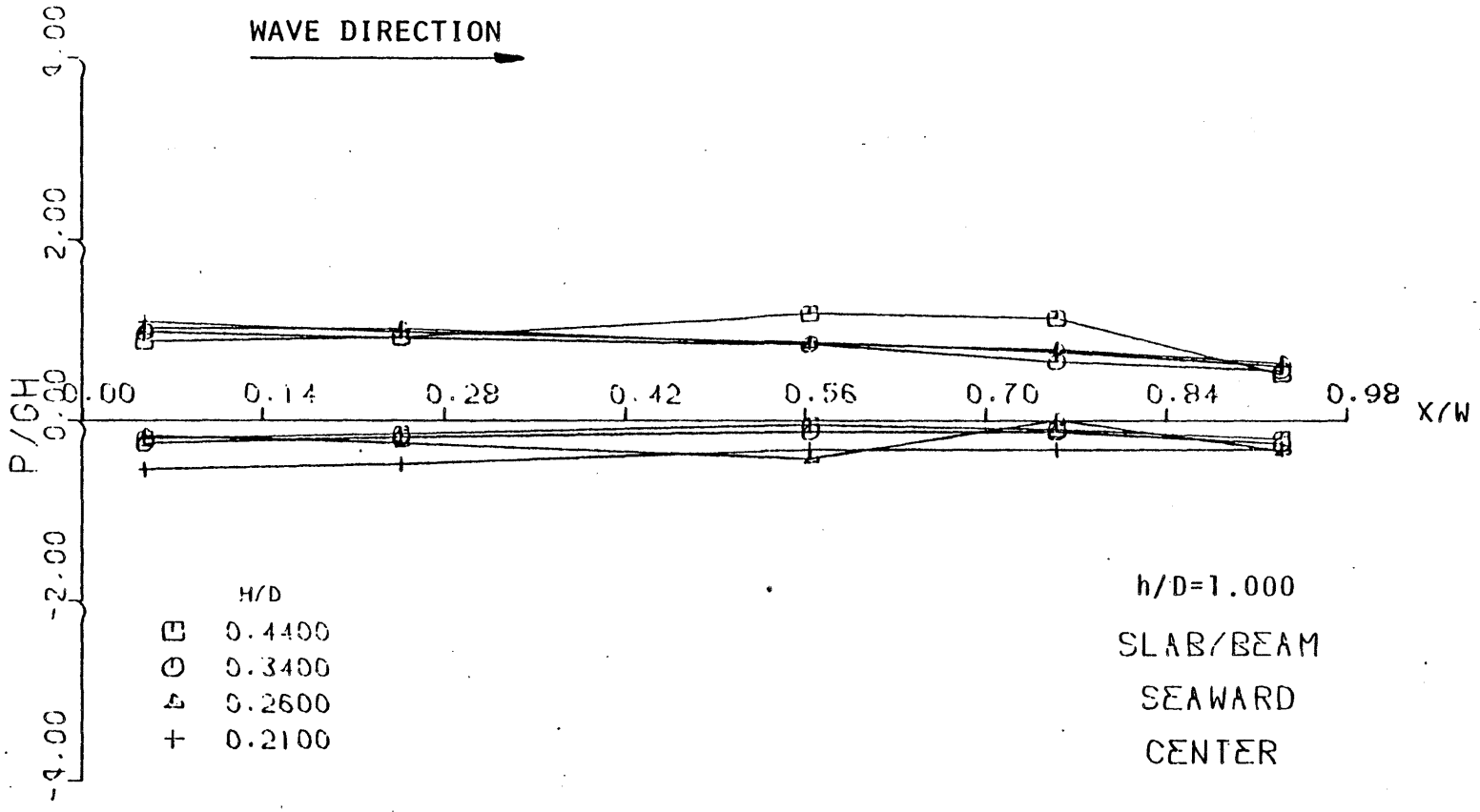

Figure 3.3 Design Curve for Slab/Beam Bridge

The prototype values are:

$+ p = 1.00 \times 64.0 \times 8.8 = + 563$ PSF

$- p = 0.2 \times 64.0 \times 8.8 = - 113$ PSF

No particularly significant change is noted for this case either transverse to the bridge nor between the midspan line and the transverse line near the supports.

It must be remembered that these pressures are peak pressures and do not occur simultaneously on the bridge although the time interval between peaks at various locations is quite short.

The quantities obtained from the design curves represent only pressures and suctions on the bottom surface of the bridge. In addition, the designer will require the hydrostatic pressure due to wave overwash for the design of the bridge slabs and beams. The theoretical overwash is obtained as:

$$H_T = 2/3\ H + D - h$$

$$H_T = \frac{2}{3} \times 8.8 + 22 - 22 = 5.87'$$

H_T represents the height of an unaltered wave form above the slab of the slab/beam bridge.

From equation 3-2:

$$H_0/h = 1.19\ H_T/h + 0.829\ h/D - 0.754$$

where H_0 is the actual wave height above the top of the slab on the seaward lanes. For the example:

$H_0/h = 1.19 \times (+5.87)/22 + 0.829 \times 22/22 - 0.754$

$H_0/h = 0.392$

$H_0 = 0.392 \times 22' = 8.62'$

The hydrostatic pressure caused by wave overwash in salt water is 8.62' x 64.0 = 552 PSF near the seaward edge and diminishing somewhat near the landward edge of the seaward lanes. The total downward pressure on the slab consists of the hydrostatic pressure of the wave overwash of 552 PSF and the bottom suction of 113 PSF for a total of 665 PSF downward and a bottom pressure of 563 PSF upward. The next question to be addressed concerns the existence of the pressures in combination. During the passage of a wave across the bridge structure, the following observations were made. The positive bottom pressure upward always occurs first at every point along the underside of the bridge, followed by the suction signal. This is thought to be caused by the movement of a suppressed crest followed by the "pulling" away during the trough passage. In cases where wave overwash occurs the water flows over the top of the bridge to the landward side of the landward lanes of the slab/beam bridge in a form completely different from the original wave form. The wave overwash could persist through the entire wave cycle or for short period waves coupled with a wide structure several cycles of wave action could occur during the persistence of overwash from the first wave of a series. Because of this effect, the author believes wave overwash should be used in combination with bottom pressures to produce maximum possible loadings.

The largest dimensionless pressures observed for the slab/beam bridge were +4.0 and -1.8 occurring at h/D = 1.222 (Figure B.5, Appendix B). The corresponding prototype water depth is 18 feet and the maximum wave height attainable was H = 8.1 feet for the prototype. The calculation of prototype pressures for these conditions gives for salt water:

$$p = +2073 \text{ pounds/sq. ft.}$$

and

$$p = -932 \text{ pounds/sq. ft.}$$

In addition to the suction pressure of -932 psf, the wave overwash is calculated as:

$$H_t = 8.1 \times 2/3 + 18.0 - 22.0 = 1.4 \text{ feet}$$

Referring to Figure 3.1 with $H_t/h = 0.06$, $H_0/h = 0.3$ and the actual overwash is 6.6 feet. The wave overwash produces an additional downward load of 64.0 x 6.6 or 422 pounds/square foot. The total downward loading is then 422 + 932 or 1354 pounds/square foot. Comparing these loads with the AASHTO Standard Specifications for Highway Bridges, 1977 (3), the heaviest lane loading listed is 640 pounds/linear foot over a 10 foot lane width or 64 pounds/square foot. Adding the dead load of a 6 1/2 inch prototype slab at 81 psf gives a total downward load of 145 psf plus the AASHTO concentrated loads of 18,000 pounds for moment or 26,000 pounds for shear.

From this comparison, it seems probable that standard loading conditions would not produce structural design values for slabs which are large enough to account for wave pressures and, indeed, design for maximum possible wave pressures may not be economically feasible.

CHAPTER IV

CONCLUSIONS AND RECOMMENDATIONS

The results of this research give an indication of peak positive and negative pressures existing at discrete points on slab/beam and box girder bridges geometrically similar to the models tested. The peak pressures shown in the design curves do not exist at the same time but are very close, temporally, for the parameters of the study. In addition to the peak pressures measured on the under-surface of the bridges, a significant additional load due to wave overwash must be carried by structural elements of the bridges. The overwash was evaluated in detail for the seaward lanes of the slab/beam bridge although this was not within the scope of the original research. The overwash characteristics for the slab/beam seaward lanes may be used as a conservative guide to the amount of overwash on the landward lanes of the slab/beam bridge and both lanes of the box girder bridge.

Because of the temporal closeness of peak positive and negative pressures on the underside of the bridges and the characteristics of overwash flow, the following recommendations are offered for structural design of slab and beam elements in addition to dead loads and buoyancy effects:

1. Upward loading consisting of peak positive pressures.

2. Downward loading consisting of peak negative pressures plus overwash hydrostatic pressures.

The further recommendation is made to place these pressures as uniform loads within each slab span and in a transverse direction to produce maximum bending moments and shears as is done with any other movable live load.

The results of this study should be useful as a design or economic parameter in evaluating the effect of severe waves on local structural elements of coastal bridges.

Bibliography

1. Keith H. Denson, Wave Forces on Causeway-Type Coastal Bridges, Water Resources Research Institute, Mississippi State University, Mississippi State, Mississippi, October 1978.

2. Keith H. Denson, Wave Forces on Causeway-Type Coastal Bridges: Effects of Angle of Wave Incidence and Cross-Section Shape, Final Report, Project: MSHD-RD-80-070, Mississippi State Highway Department, Jackson, Mississippi, December 1980.

3. Standard Specifications for Highway Bridges, American Association of State Highway and Transportation Officials, Twelfth Edition, 1977.

Appendix A: Data Reduction and Computer Plotting Program

```
      REAL LENGTH
      DIMENSION B(10)
      DIMENSION D(10),E(10)
      DIMENSION Y(10), X(10),F(10)
      DIMENSION G(10), H(10), P(10)
      DIMENSION Q(10),R(10),S(10),T(10)
      READ(5,100)  CEND
      READ(5,100)  K
      J=K/2
      READ(5,100)W,C,Z
      READ(5,100)(Y(I),I=1,6)
      READ(5,100)(E(I),I=1,6)
      READ(5,100)(F(I),I=1,6)
      READ(5,100)(G(I),I=1,6)
      READ(5,100)(H(I),I=1,6)
      READ(5,100)(P(I),I=1,6)
      IF (J.EQ.3) GO TO 2
      READ(5,100)(Q(I),I=1,6)
      READ(5,100)(R(I),I=1,6)
      IF (J.EQ.4) GO TO 2
      READ(5,100)(S(I),I=1,6)
      READ(5,100)(T(I),I=1,6)
2     READ(5,100)(X(I),I=1,6)
      READ(5,100)(D(I),I=1,J)
      READ(5,100)(B(I),I=1,J)
      READ(5,100)LENGTH
100   FORMAT( )
      DO 105 I=1,6
      Y(I)=Y(I)/(62.4*B(1))
      E(I)=E(I)/(62.4*B(1))
      F(I)=F(I)/(62.4*B(2))
      G(I)=G(I)/(62.4*B(2))
      H(I)=H(I)/(62.4*B(3))
      P(I)=P(I)/(62.4*B(3))
105   CONTINUE
      IF (J.EQ.3) GO TO 13
      DO 106 I=1,6
      Q(I)=Q(I)/(62.4*B(4))
      R(I)=R(I)/(62.4*B(4))
106   CONTINUE
      IF (J.EQ.4) GO TO 13
      DO 107 I=1,6
      S(I)=S(I)/(62.4*B(5))
      T(I)=T(I)/(62.4*B(5))
107   CONTINUE
13    A=Y(5)
      U=Y(6)
      Y(5)=(64.)/(62.4*.211)
      Y(6)=(-64.)/(62.4*.211)
      DO 16 I=1,6
16    X(I)=X(I)/W
      CALL PLOTS(0,0,6)
```

```
      CALL PLOT(1.75,2.,-3)
      N=6
      CALL SCALE(X(1),7.,N,1)
      CALL SCALE(Y(1),4.,N,1)
      Y(5)=A
      Y(6)=U
      X(8)=.17
      Y(7)=-4.0
      Y(8)=2.0
      E(7)=Y(7)
      E(8)=Y(8)
      F(7)=Y(7)
      F(8)=Y(8)
      G(7)=Y(7)
      G(8)=Y(8)
      H(7)=Y(7)
      H(8)=Y(8)
      P(7)=Y(7)
      P(8)=Y(8)
      IF (J.EQ.3) GO TO 22
      Q(7)=Y(7)
      Q(8)=Y(8)
      R(7)=Y(7)
      R(8)=Y(8)
      IF (J.EQ.4) GO TO 22
      S(7)=Y(7)
      S(8)=Y(8)
      T(7)=Y(7)
      T(8)=Y(8)
22    V=(Z)/(C)
      CALL AXIS(0.,2.,' ',17.,0.,X(7),X(8))
      CALL AXIS(0.,0.,'P/GH',4,4.,90.,Y(7),Y(8))
      CALL SYMBOL(7.4,2.,.1,'X/W',0.,3)
      CALL SYMBOL(6.,1.,.1,88,0.,-1)
      CALL SYMBOL(999.,999..1,'/D=',0.,3)
      CALL NUMBER(6.39,1.,.1,V,0.,1)
      CALL SYMBOL(5.75,.7,.125,'BOX GIRDER',0.,10)
      CALL SYMBOL(5.875,.4,.125,'SEAWARD',0.,7)
      CALL SYMBOL(.90,1.,.08,'H',0.,1)
      CALL SYMBOL(999.,999.,.08,'/D',0.,2)
      CALL LINE(X,Y,N,1,1,0)
      CALL LINE(X,E,N,1,1,0)
      CALL LINE(X,F,N,1,1,1)
      CALL LINE (X,G,N,1,1,1)
      CALL LINE (X,H,N,1,1,2)
      CALL LINE (X,P,N,1,1,2)
      IF(J.EQ.3) GO TO 21
      CALL LINE(X,Q,N,1,1,3)
      CALL LINE(X,R,N,1,1,3)
      IF(J.EQ.4) GO TO 21
      CALL LINE(X,S,N,1,1,4)
      CALL LINE(X,T,N,1,1,4)
21    NN=-1
```

```
      YOR=.93
      DO 19 I=1,J
      NN=NN+1
      YOR=YOR-.2
      YSY=YOR+.05
      CALL SYMBOL(.50,YSY,.1,NN,0.,-1)
19    CALL NUMBER(.80,YOR,.1,D(I),0.,4)
      IF (CEND.LT.0.0) GO TO 25
      CALL SYMBOL(5.9,.1,.125,'CENTER',0.,6)
      GO TO 26
 25   CALL SYMBOL(5.9,.1,.125,'NEAR END',0.,8)
26    CALL PLOT(0.,0.,999)
      STOP
      END
```

Appendix B: Design Curves for Slab/Beam Bridge

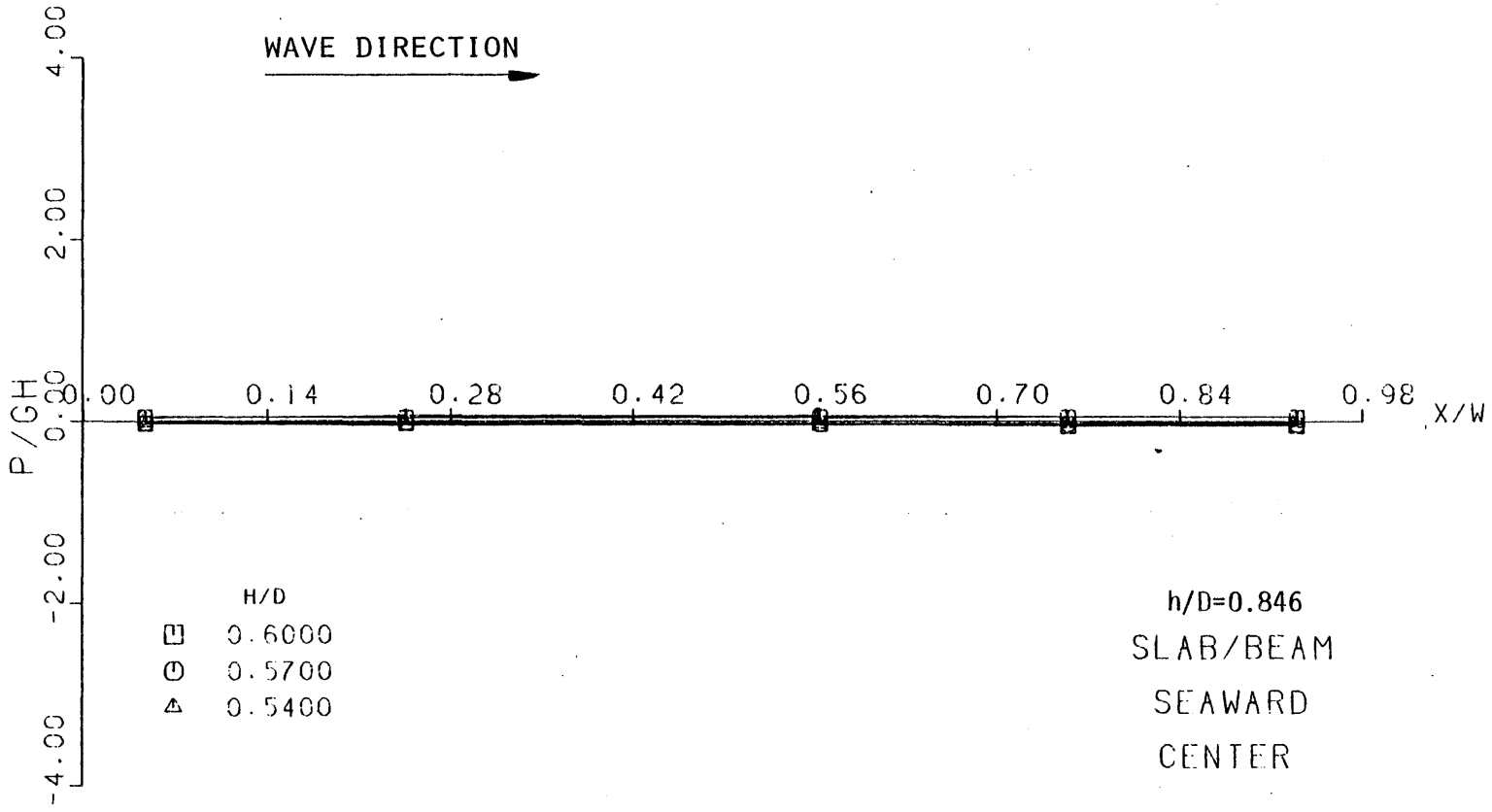
WAVE DIRECTION
4.00
2.00
0.00
-2.00
-4.00
P/GH
0.00
0.14
0.28
0.42
0.56
0.70
0.84
0.98
X/W
H/D
0.6000
0.5700
0.5400
h/D=0.846
SLAB/BEAM
SEAWARD
CENTER

Figure B.1

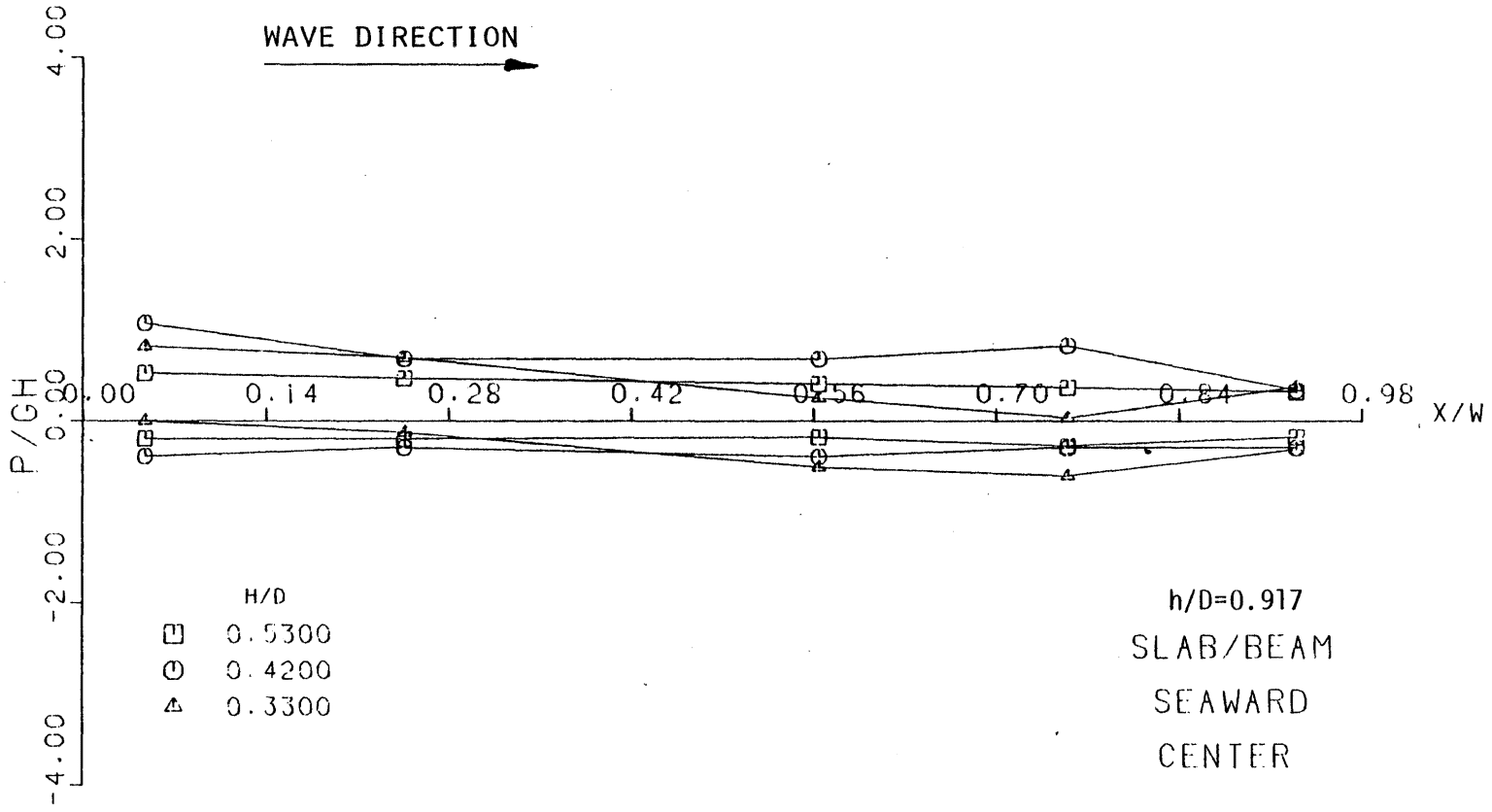
WAVE DIRECTION
4.00
2.00
0.00
-2.00
-4.00
P/GH
0.00
0.14
0.28
0.42
0.56
0.70
0.84
0.98
X/W
H/D
0.5300
0.4200
0.3300
h/D=0.917
SLAB/BEAM
SEAWARD
CENTER

Figure B.2

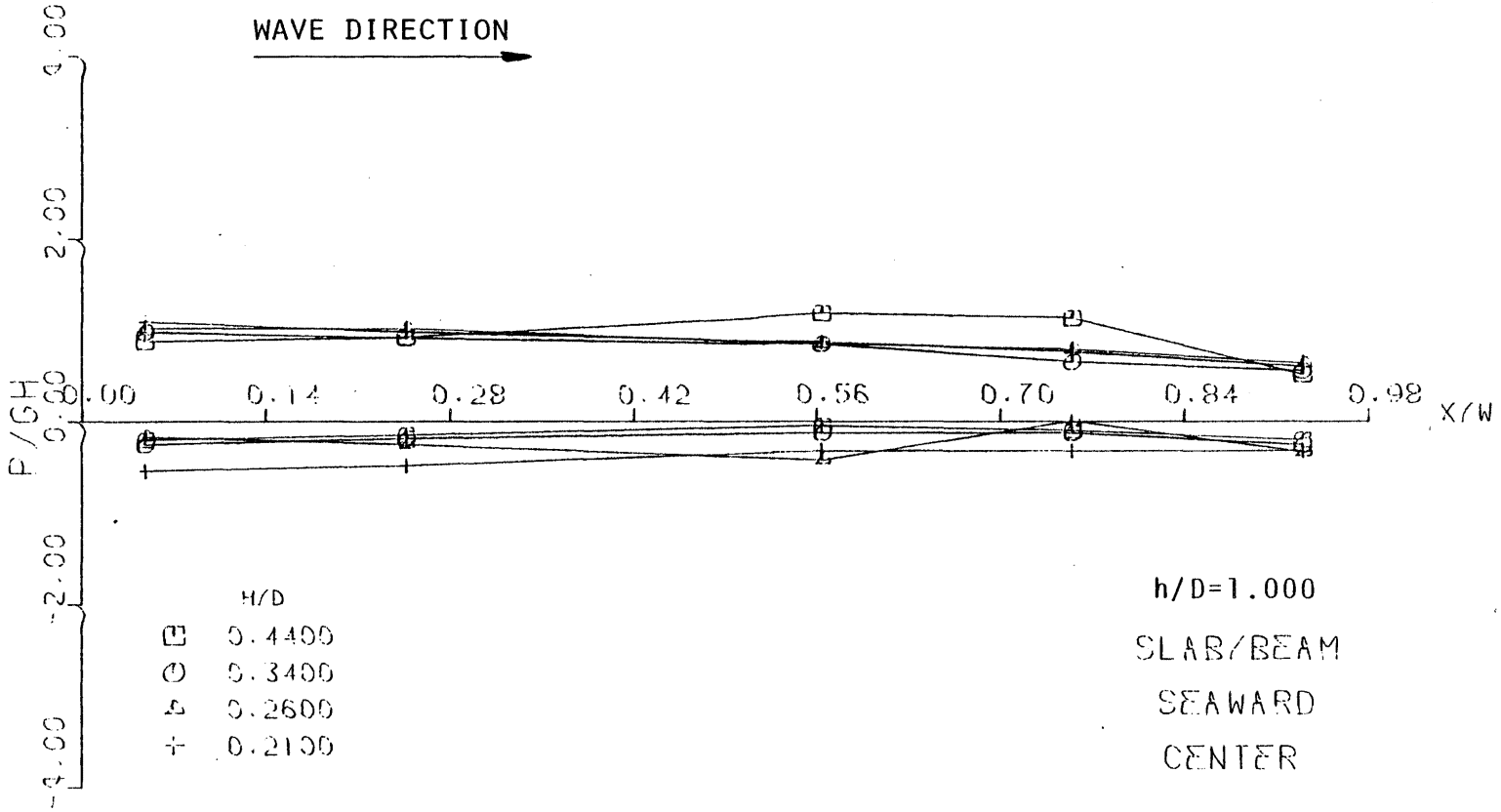

Figure B.3

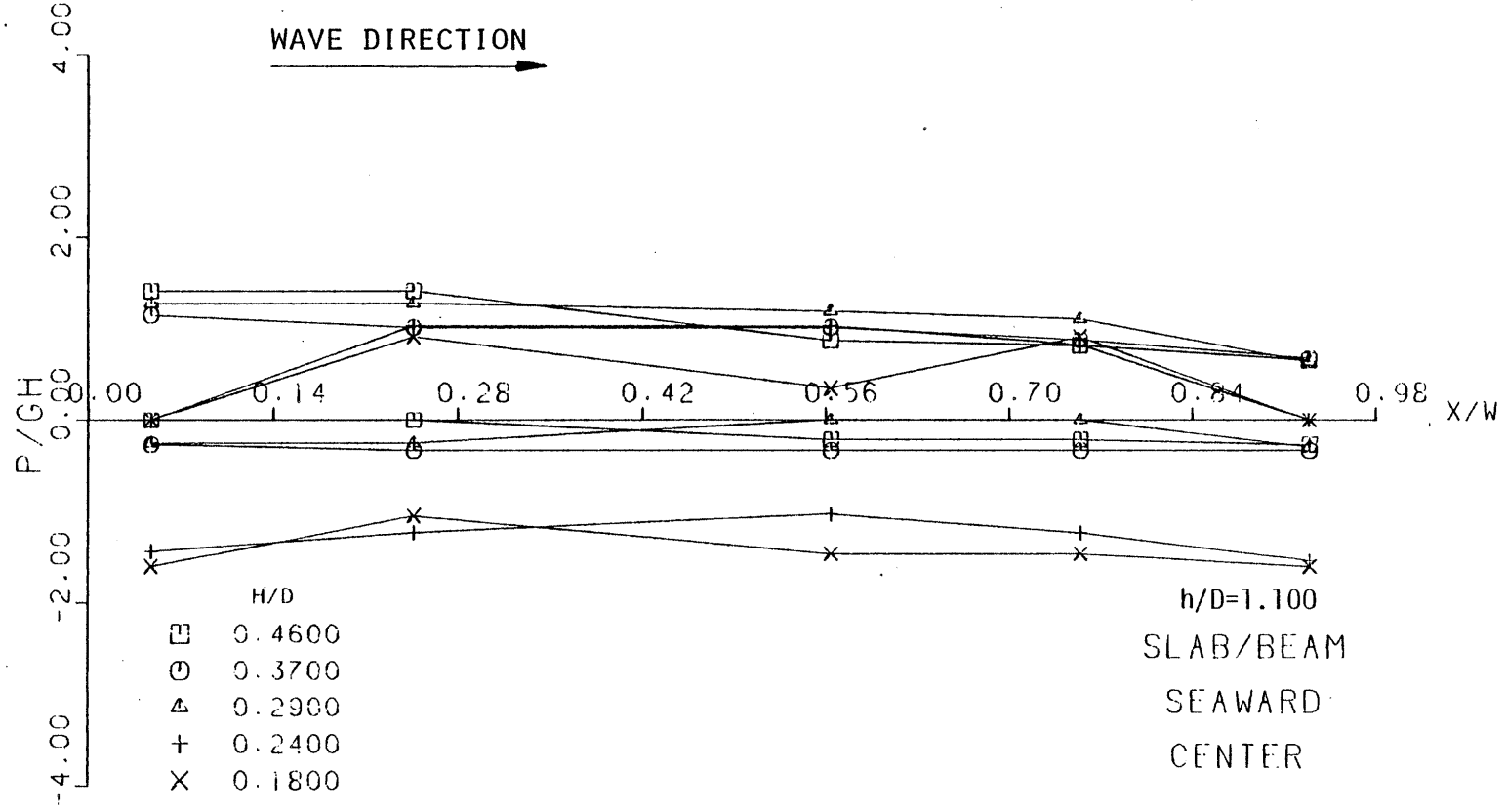
WAVE DIRECTION
4.00
2.00
0.00
-2.00
-4.00
P/GH
0.00
0.14
0.28
0.42
0.56
0.70
0.84
0.98
X/W
H/D
0.4600
0.3700
0.2900
0.2400
0.1800
h/D=1.100
SLAB/BEAM
SEAWARD
CENTER

Figure B.4

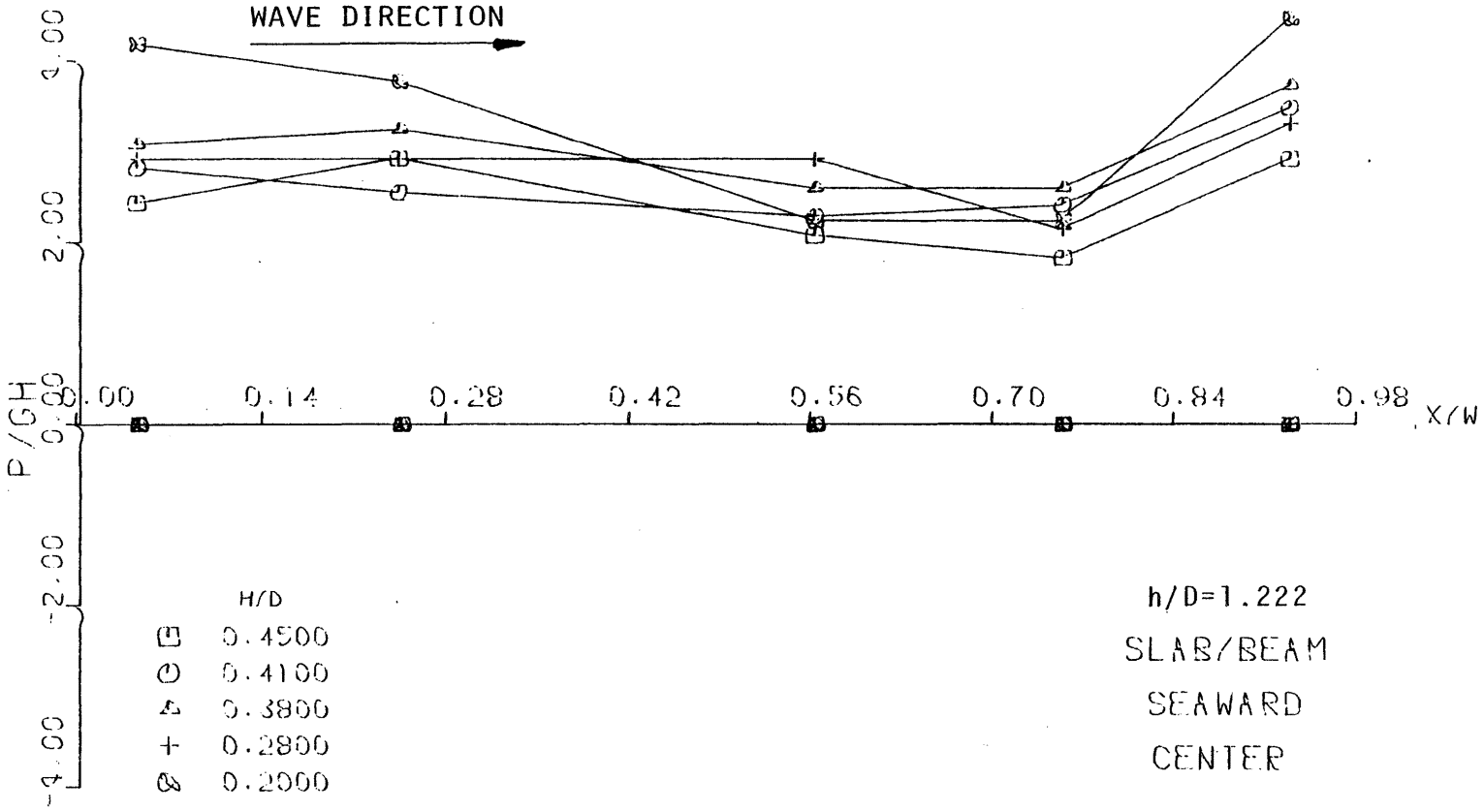

Figure B.5

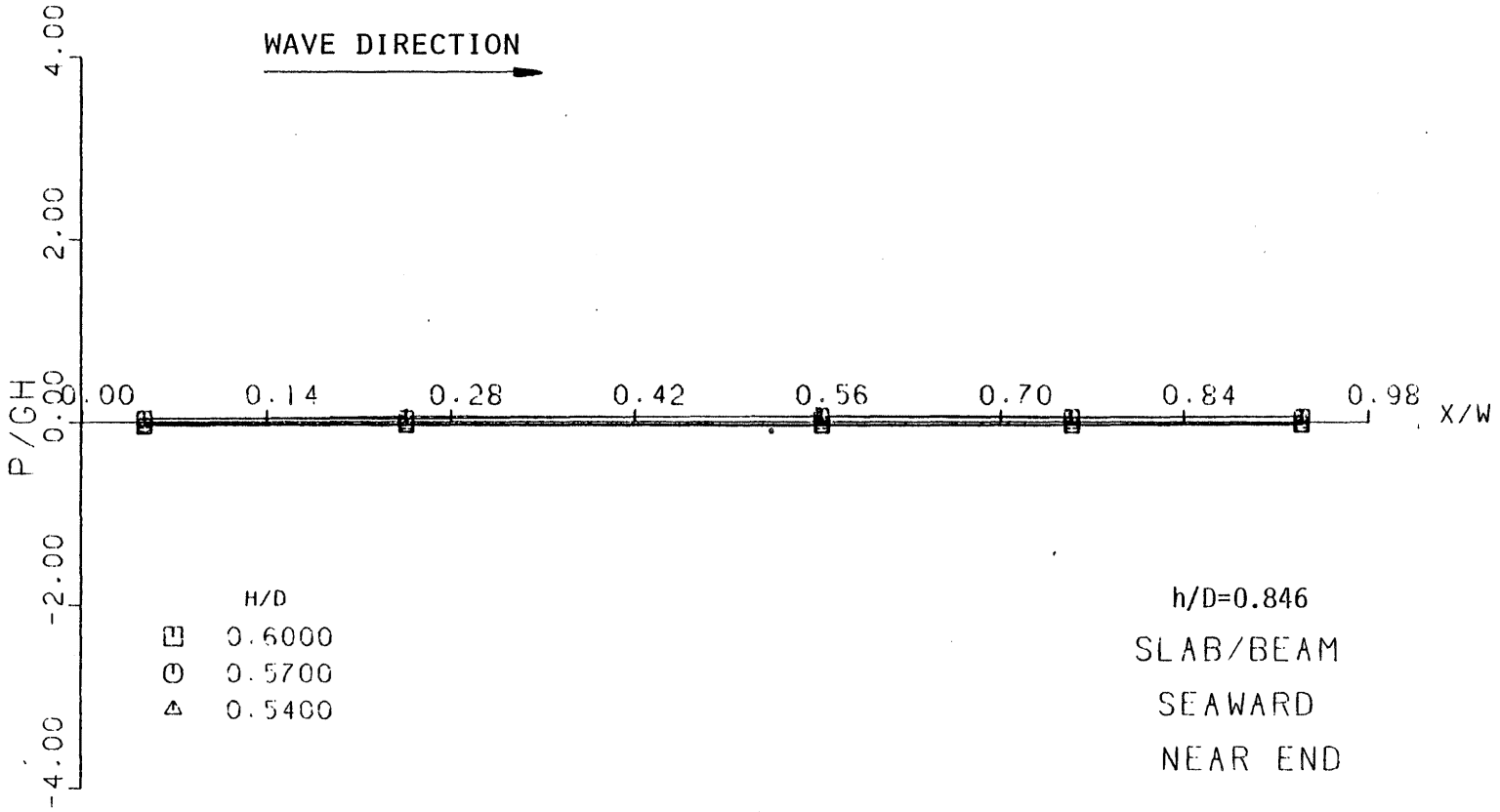
WAVE DIRECTION
4.00
2.00
0.00
-2.00
-4.00
P/GH
0.00
0.14
0.28
0.42
0.56
0.70
0.84
0.98
X/W
H/D
0.6000
0.5700
0.5400
h/D=0.846
SLAB/BEAM
SEAWARD
NEAR END

Figure B.6

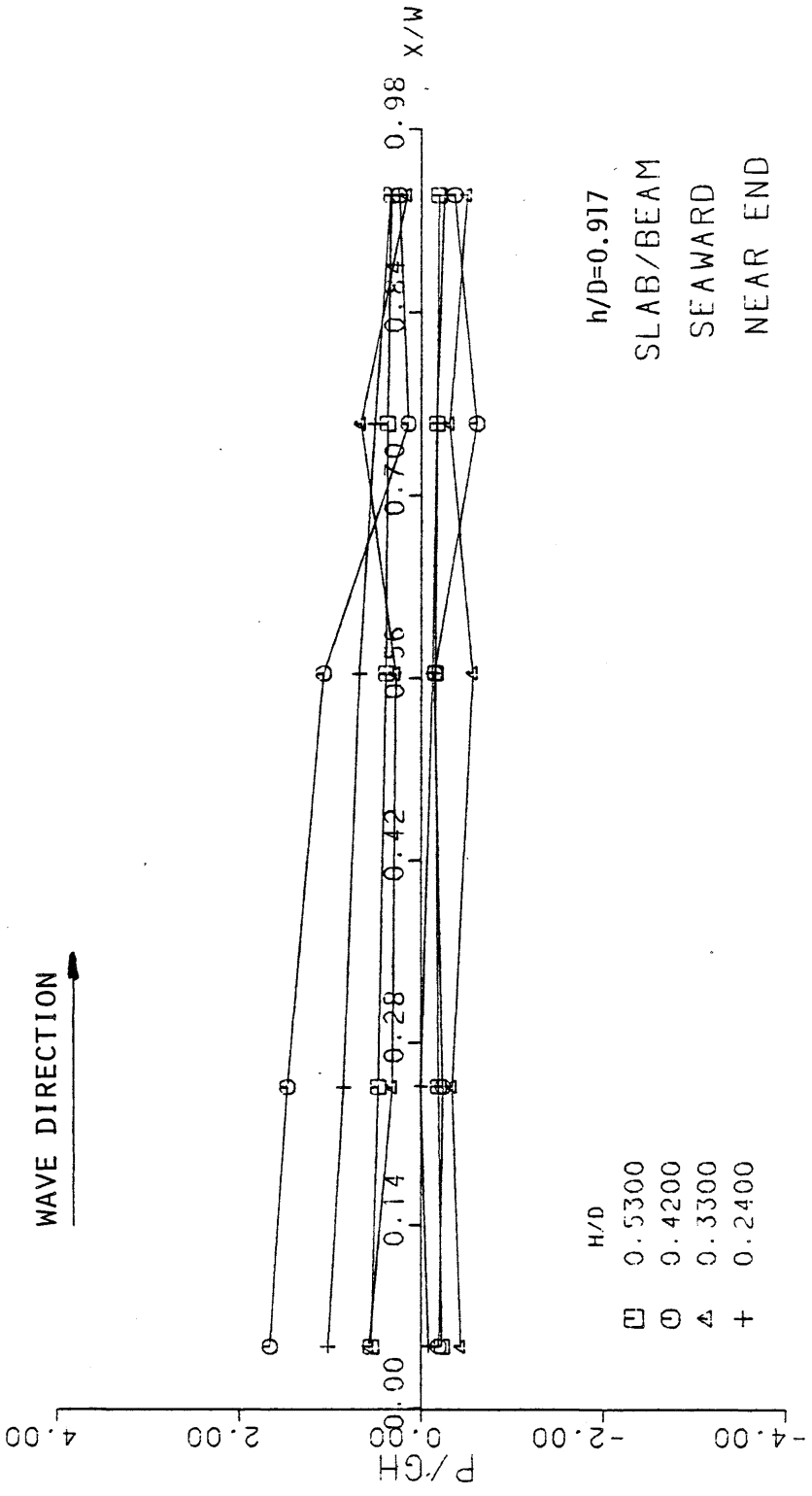
WAVE DIRECTION
P/GH
4.00
2.00
0.00
-2.00
-4.00
0.00
0.14
0.28
0.42
0.56
0.70
0.84
0.98
X/W
h/D=0.917
SLAB/BEAM
SEAWARD
NEAR END
H/D
0.5300
0.4200
0.3300
0.2400

Figure B.7

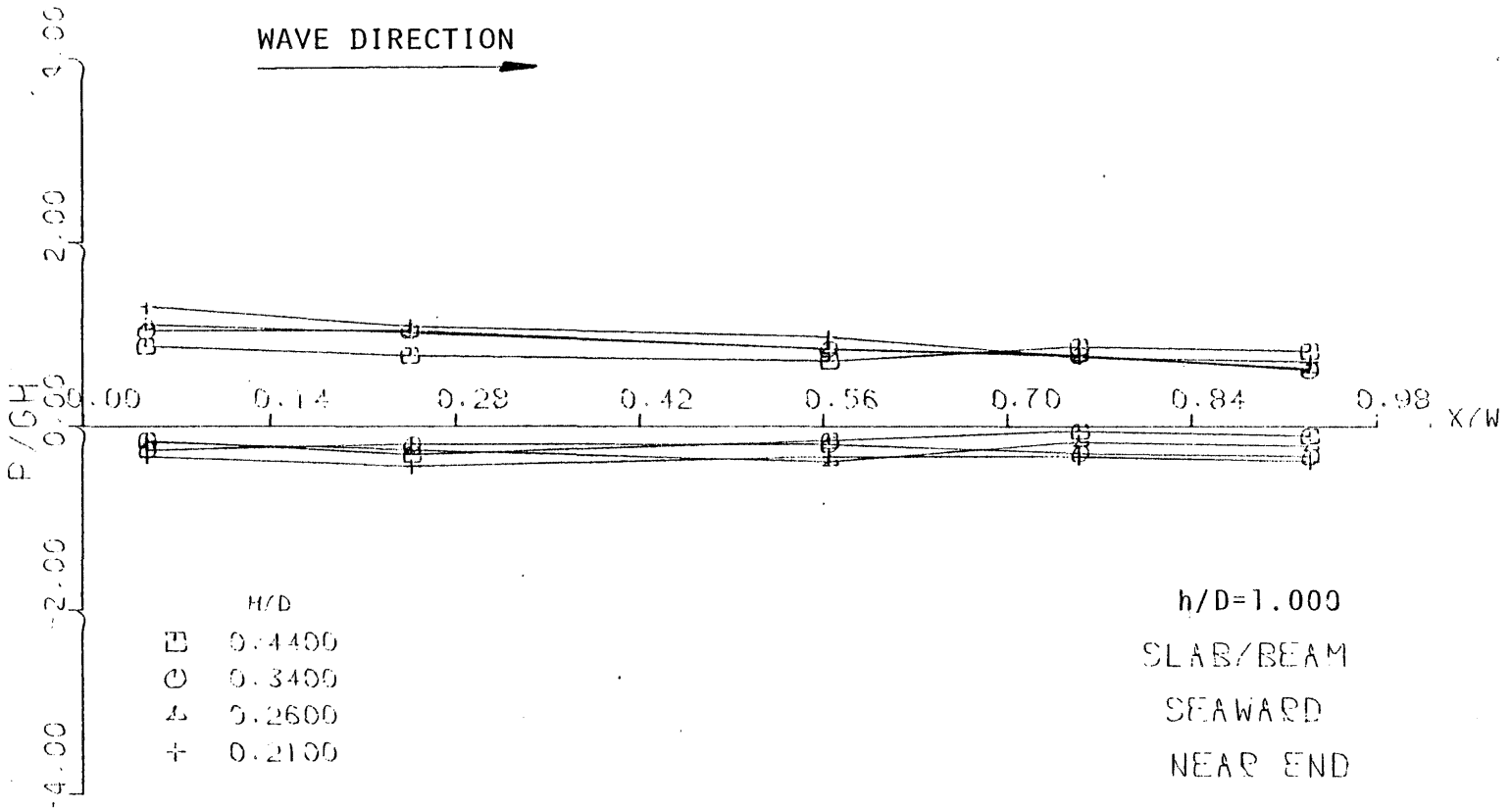

Figure B.8

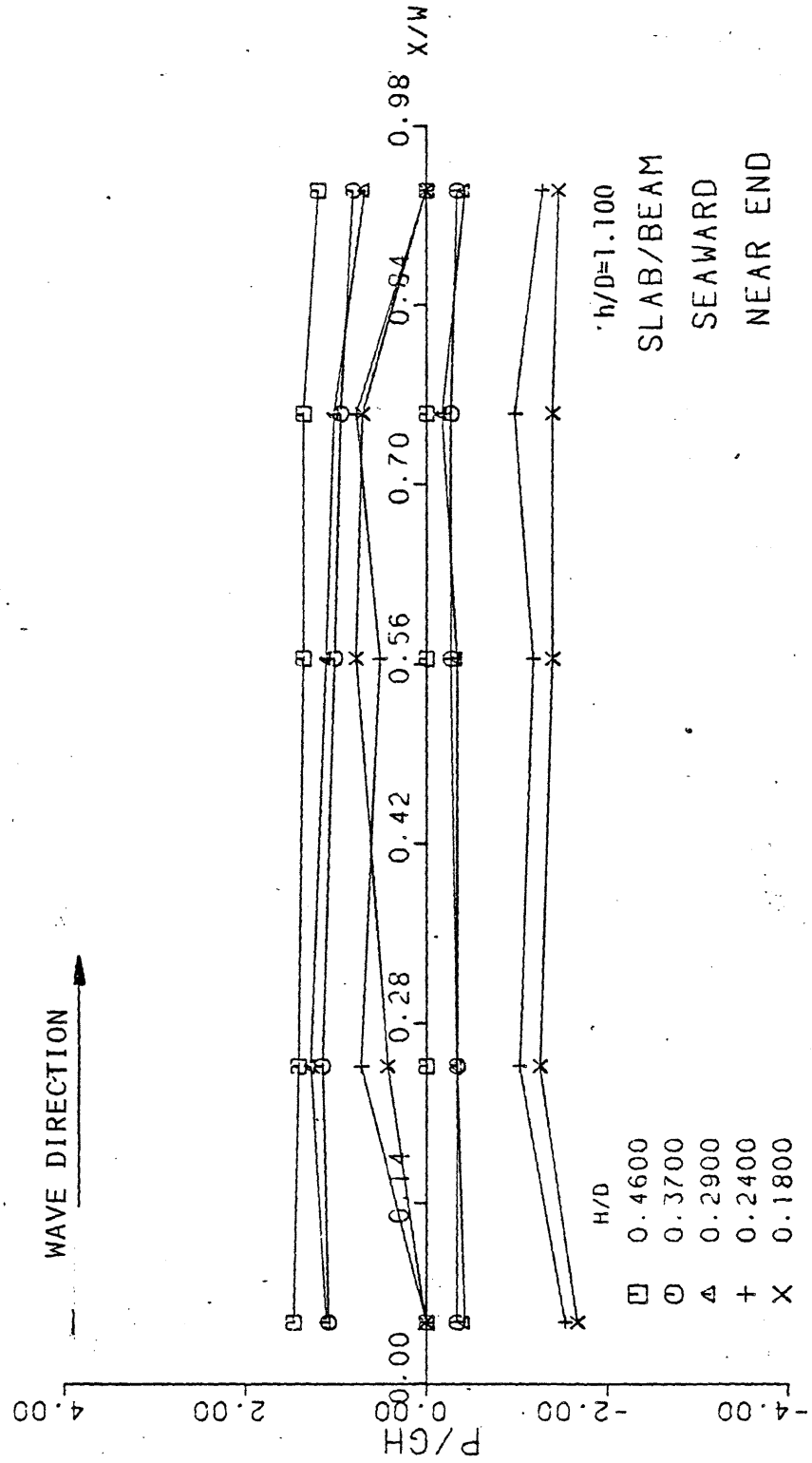
WAVE DIRECTION
P/GH
4.00
2.00
0.00
-2.00
-4.00
0.00
0.14
0.28
0.42
0.56
0.70
0.84
0.98
X/W
h/D=1.100
SLAB/BEAM
SEAWARD
NEAR END
H/D
0.4600
0.3700
0.2900
0.2400
0.1800

Figure B.9

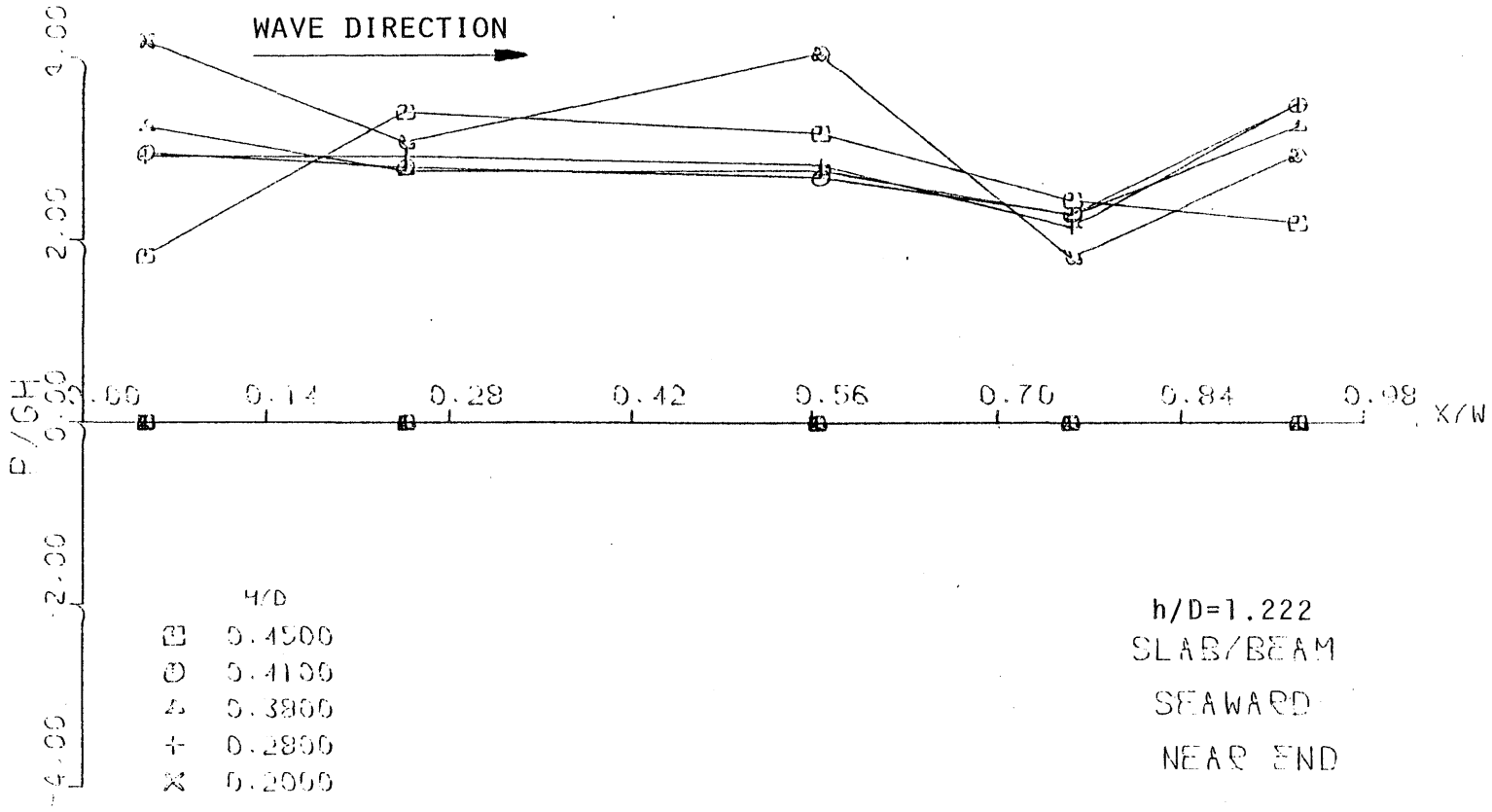

Figure B.10

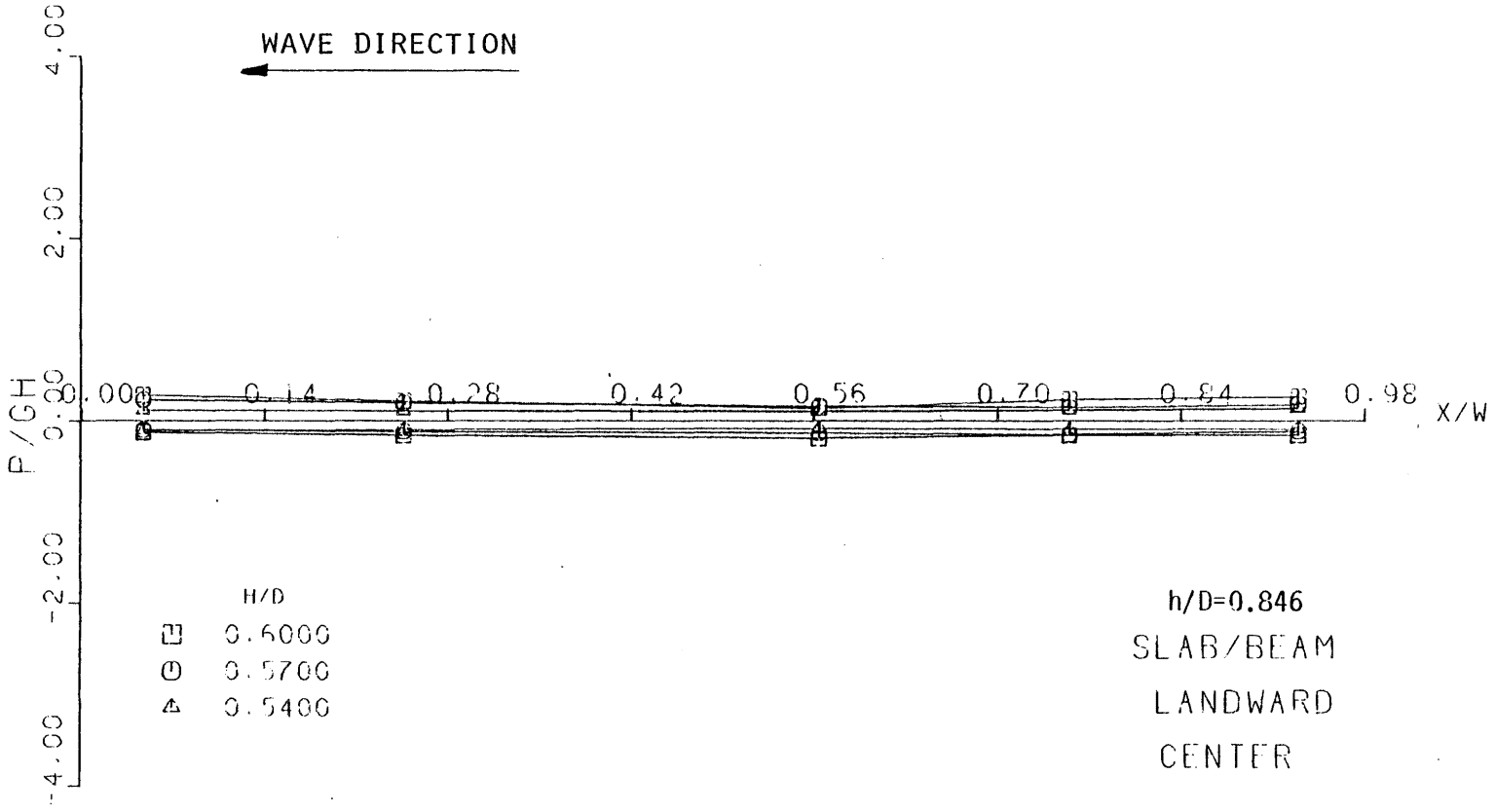
WAVE DIRECTION
4.00
2.00
0.00
-2.00
-4.00
P/GH
0.00
0.14
0.28
0.42
0.56
0.70
0.84
0.98
X/W
H/D
0.6000
0.5700
0.5400
h/D=0.846
SLAB/BEAM
LANDWARD
CENTER

Figure B.11

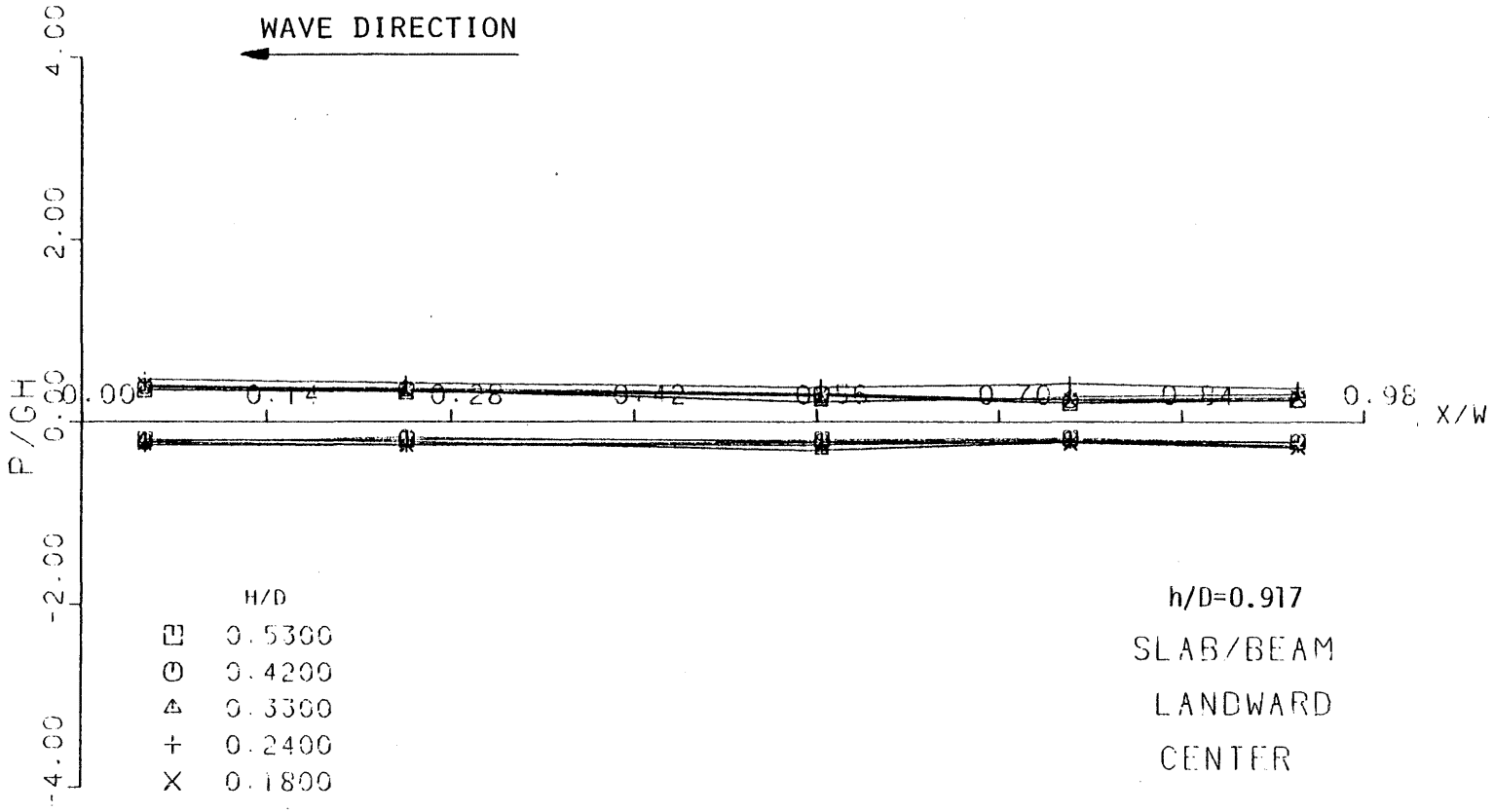
WAVE DIRECTION
4.00
2.00
0.00
-2.00
-4.00
P/GH
0.00
0.14
0.28
0.42
0.70
0.98
X/W
H/D
0.5300
0.4200
0.3300
0.2400
0.1800
h/D=0.917
SLAB/BEAM
LANDWARD
CENTER

Figure B.12

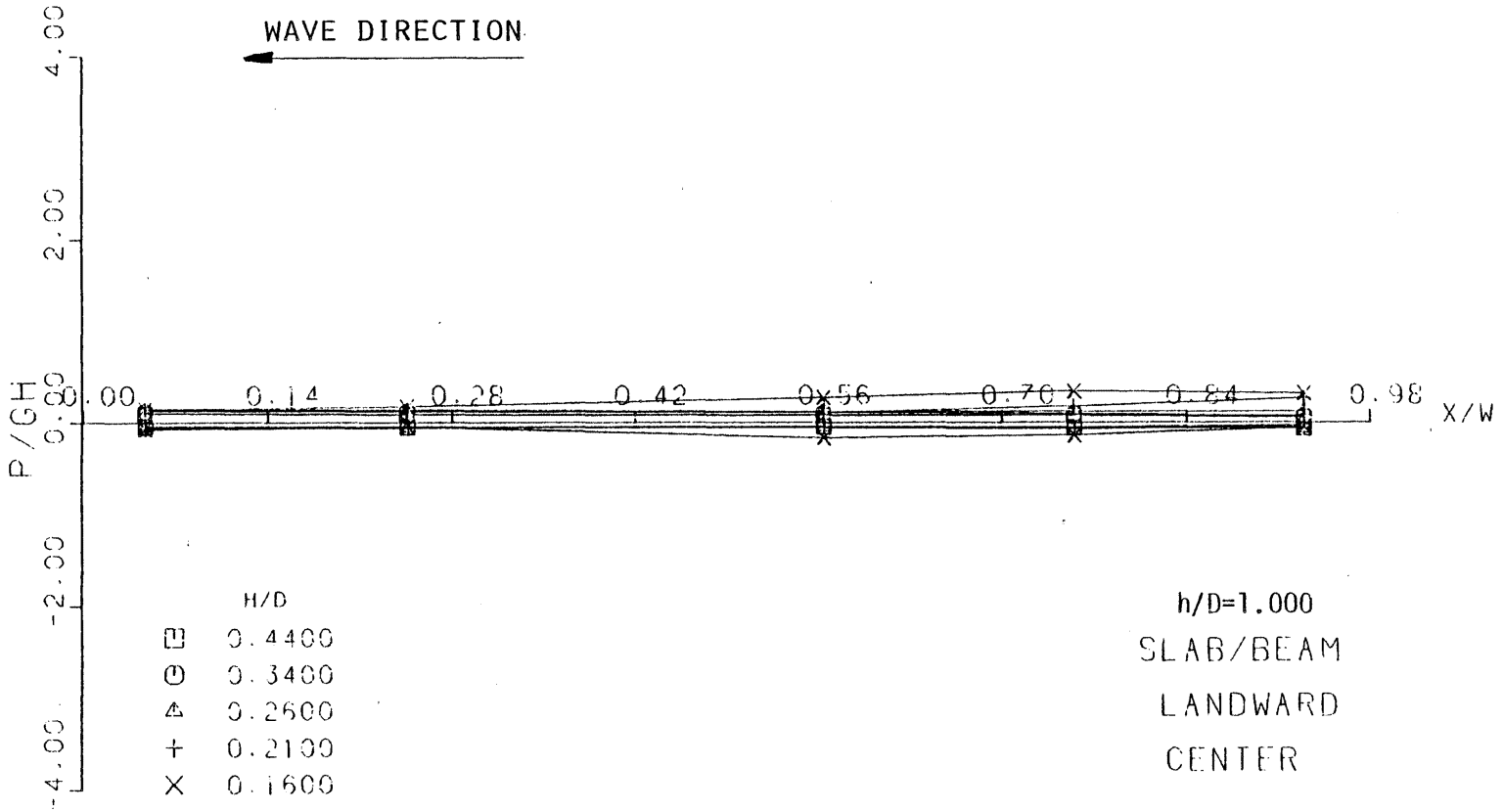
WAVE DIRECTION
4.00
2.00
0.00
-2.00
-4.00
P/GH
0.00
0.14
0.28
0.42
0.56
0.70
0.84
0.98
X/W
H/D
0.4400
0.3400
0.2600
0.2100
0.1600
h/D=1.000
SLAB/BEAM
LANDWARD
CENTER

Figure B.13

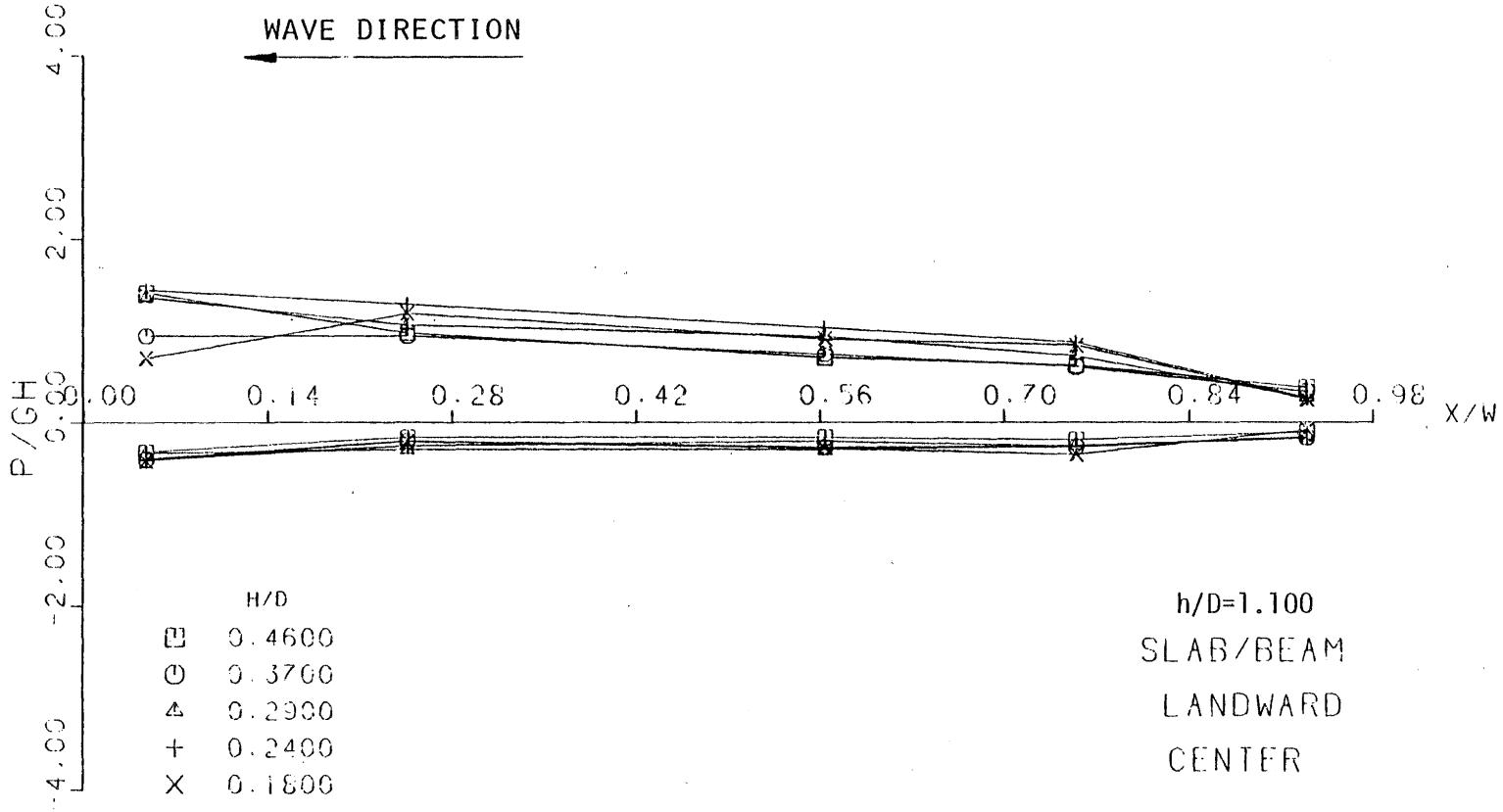
WAVE DIRECTION
4.00
2.00
0.00
-2.00
-4.00
P/GH
0.00
0.14
0.28
0.42
0.56
0.70
0.84
0.98
X/W
H/D
0.4600
0.3700
0.2900
0.2400
0.1800
h/D=1.100
SLAB/BEAM
LANDWARD
CENTER

Figure B.14

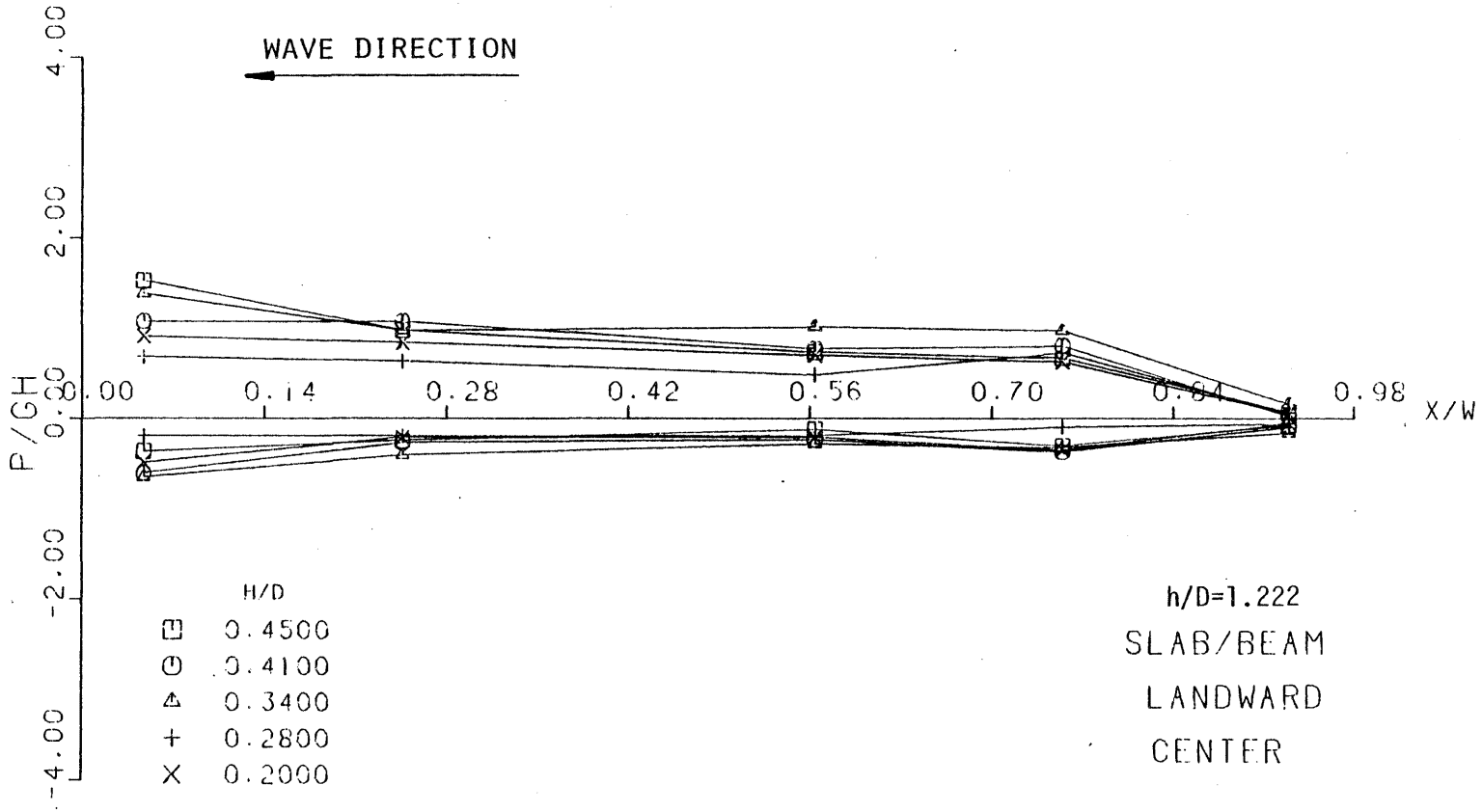
WAVE DIRECTION
4.00
2.00
0.00
-2.00
-4.00
P/GH
0.00
0.14
0.28
0.42
0.56
0.70
0.84
0.98
X/W
H/D
0.4500
0.4100
0.3400
0.2800
0.2000
h/D=1.222
SLAB/BEAM
LANDWARD
CENTER

Figure B.15

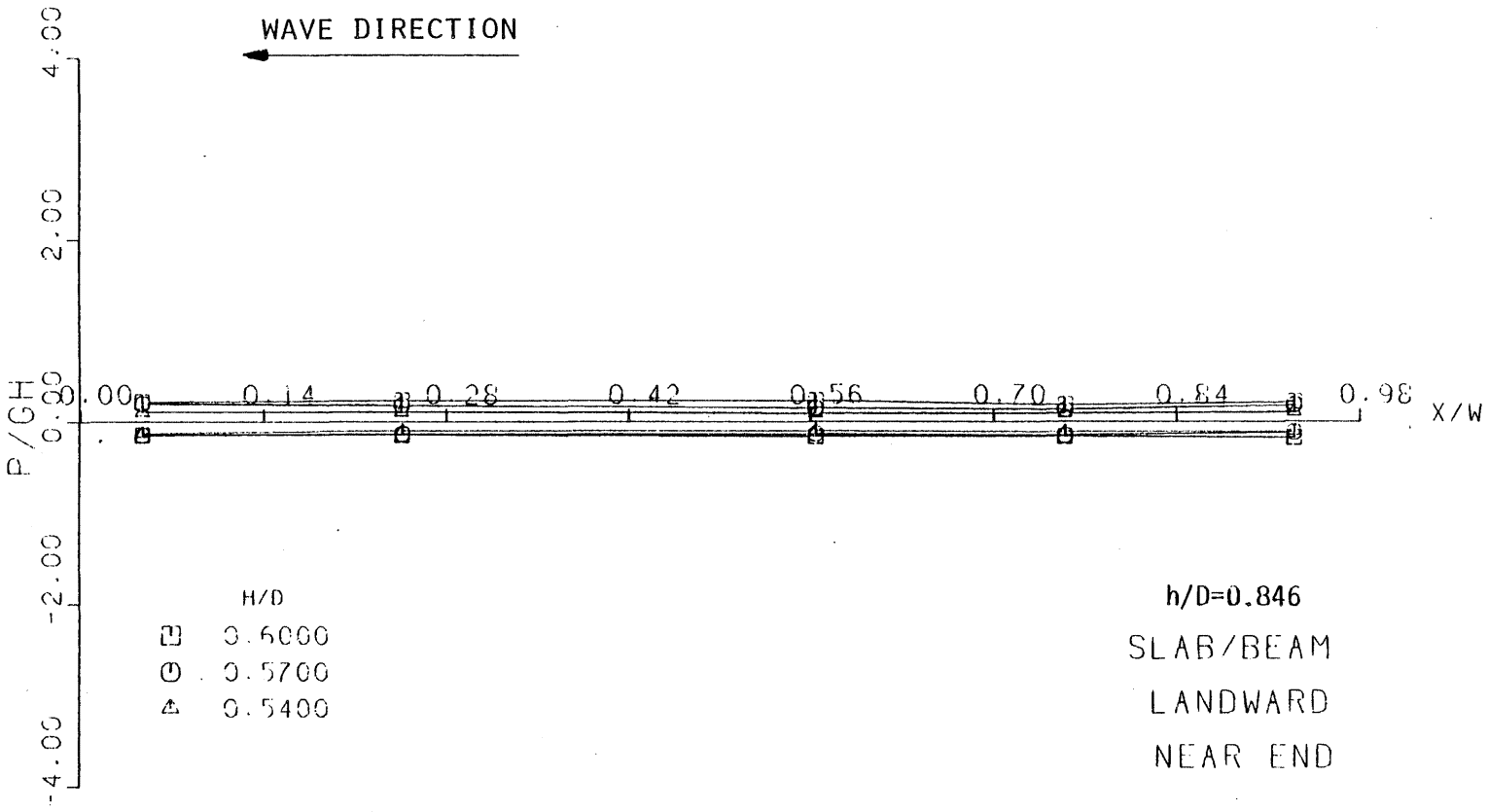
WAVE DIRECTION
4.00
2.00
0.00
-2.00
-4.00
P/GH
0.00
0.14
0.28
0.42
0.56
0.70
0.84
0.98
X/W
H/D
0.6000
0.5700
0.5400
h/D=0.846
SLAB/BEAM
LANDWARD
NEAR END

Figure B.16

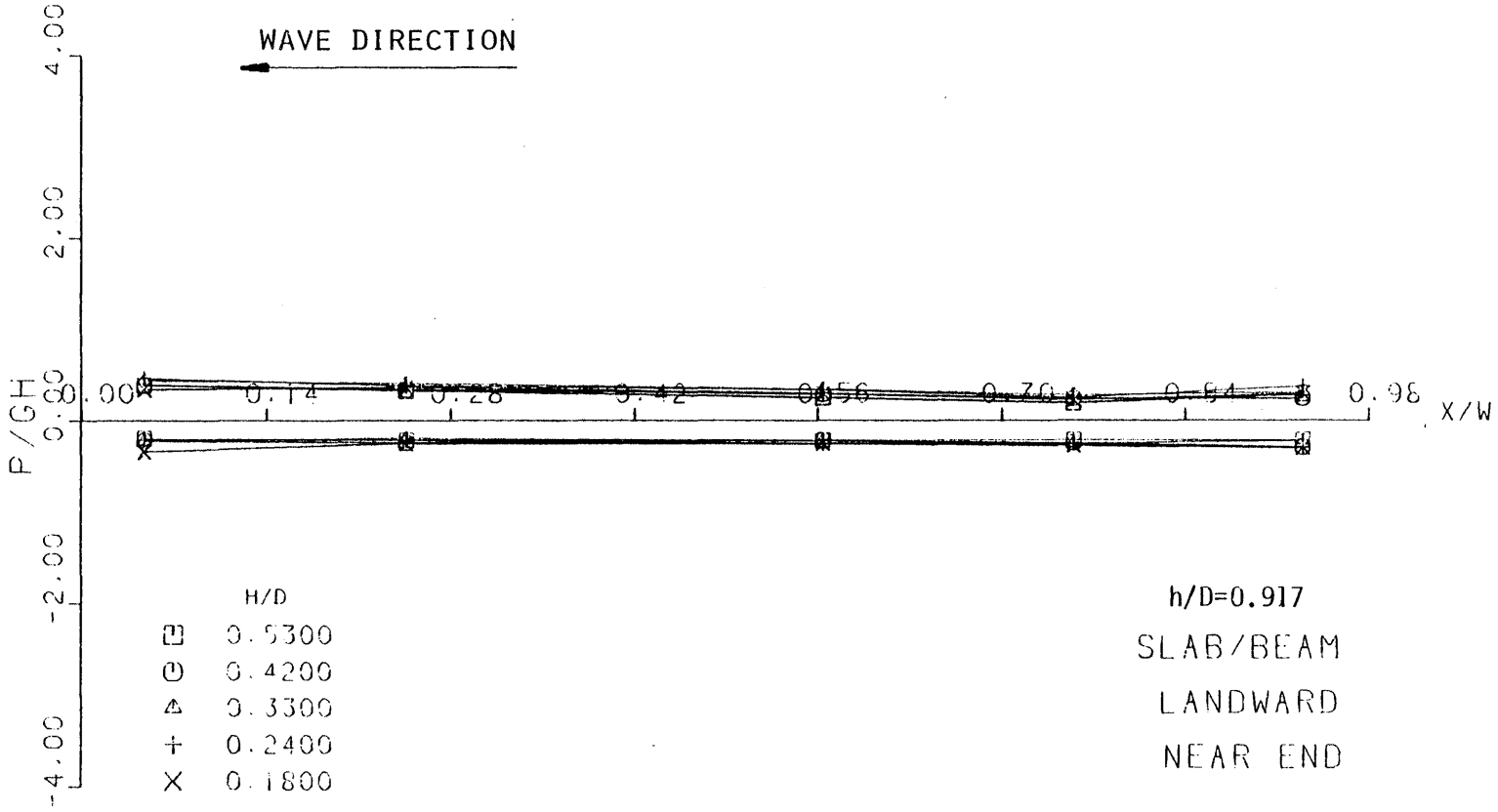
WAVE DIRECTION
4.00
2.00
0.00
-2.00
-4.00
P/GH
0.00
0.14
0.28
0.42
0.56
0.70
0.84
0.98
X/W
H/D
0.5300
0.4200
0.3300
0.2400
0.1800
h/D=0.917
SLAB/BEAM
LANDWARD
NEAR END

Figure B.17

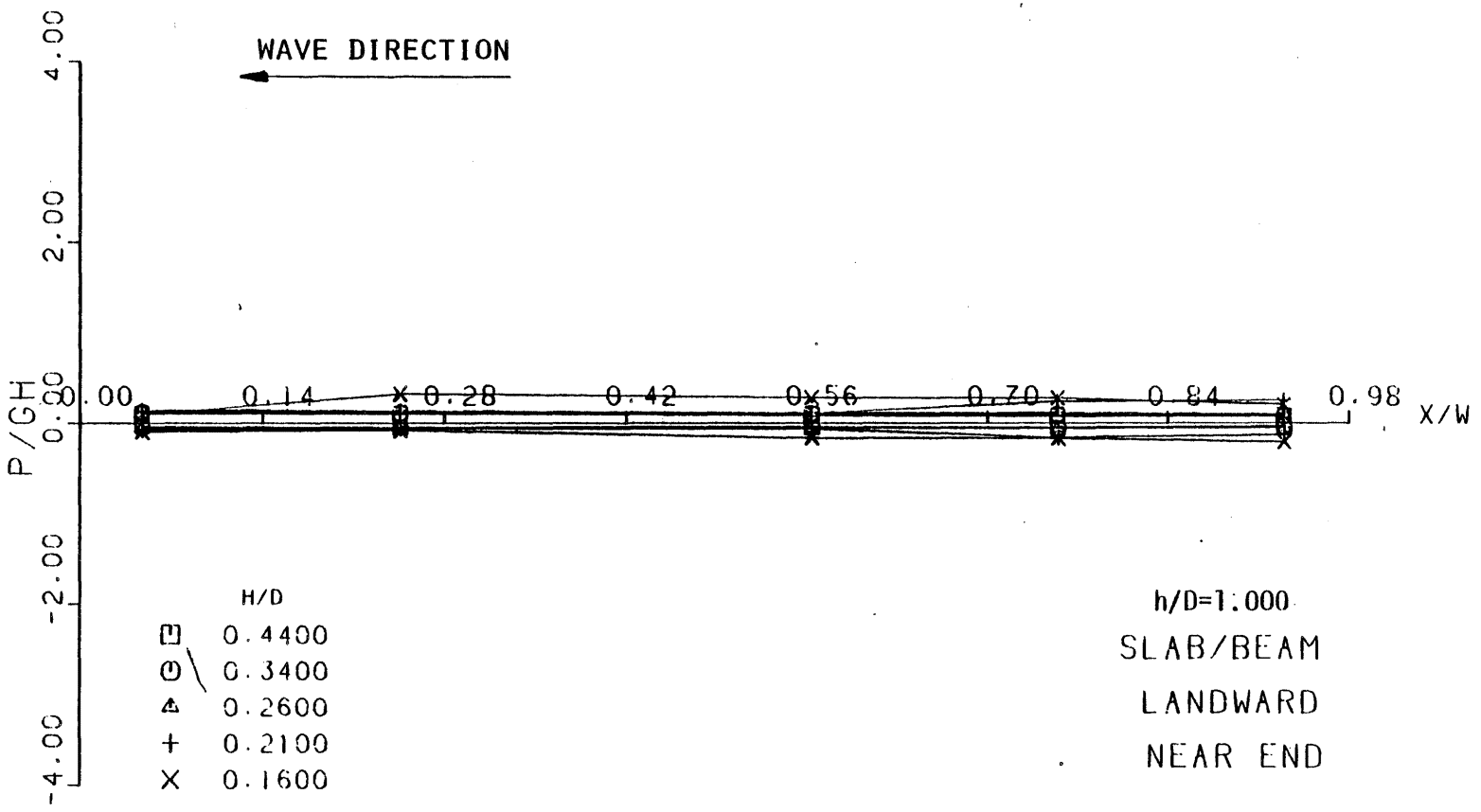
WAVE DIRECTION
4.00
2.00
0.00
-2.00
-4.00
P/GH
0.00
0.14
0.28
0.42
0.56
0.70
0.84
0.98
X/W
H/D
0.4400
0.3400
0.2600
0.2100
0.1600
h/D=1.000
SLAB/BEAM
LANDWARD
NEAR END

Figure B.18

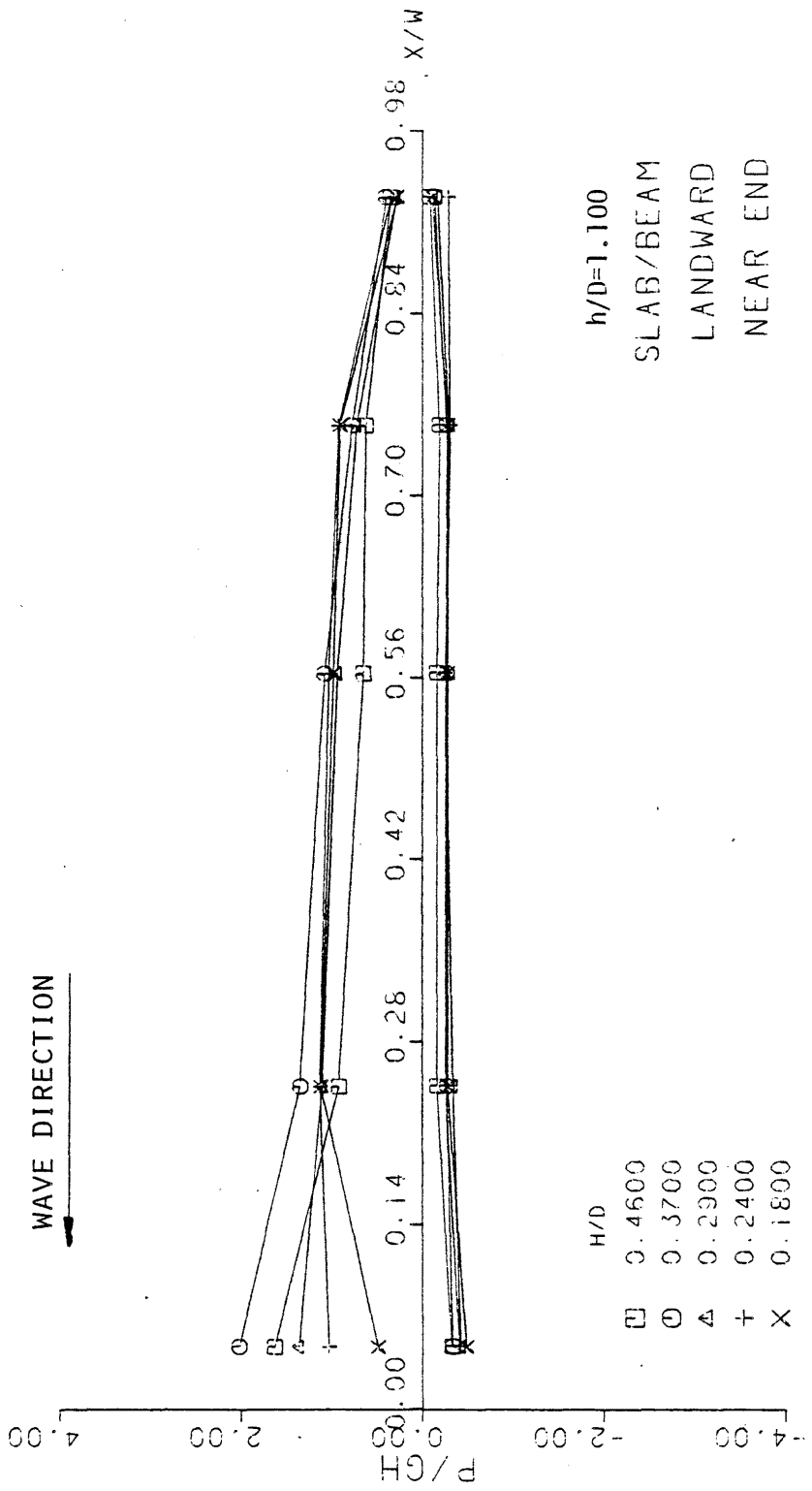
WAVE DIRECTION
P/GH
X/W
0.00
0.14
0.28
0.42
0.56
0.70
0.84
0.98
4.00
2.00
0.00
-2.00
-4.00
h/D=1.100
SLAB/BEAM
LANDWARD
NEAR END
H/D
0.4600
0.3700
0.2300
0.2400
0.1800

Figure B.19

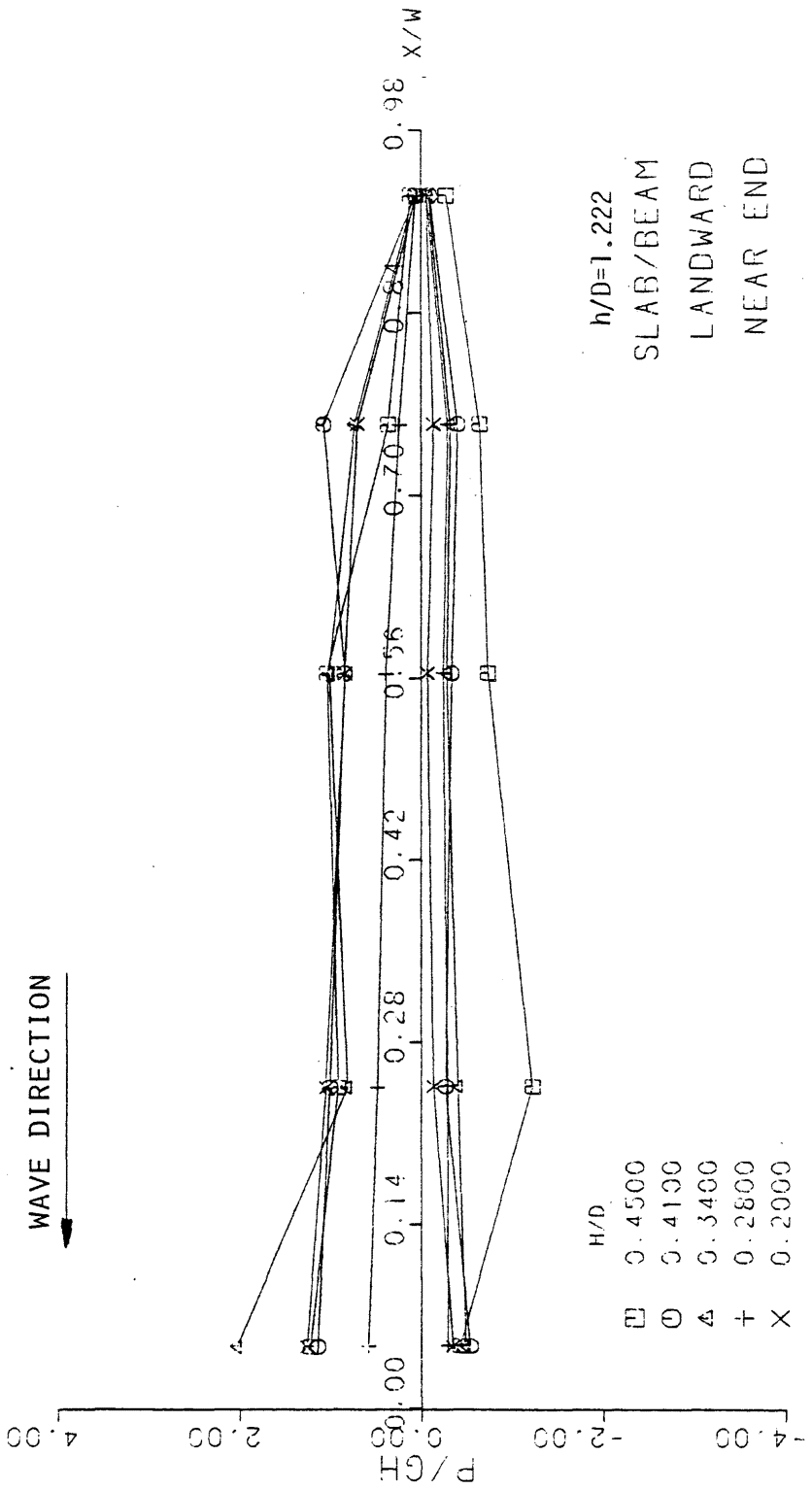
WAVE DIRECTION
P/GI
4.00
2.00
0.00
-2.00
-4.00
0.00
0.14
0.28
0.42
0.56
0.70
0.84
0.98
X/W
h/D=1.222
SLAB/BEAM
LANDWARD
NEAR END
H/D
0.4500
0.4130
0.3400
0.2800
0.2000

Figure B.20

Appendix C: Design Curves for Box Girder Bridge

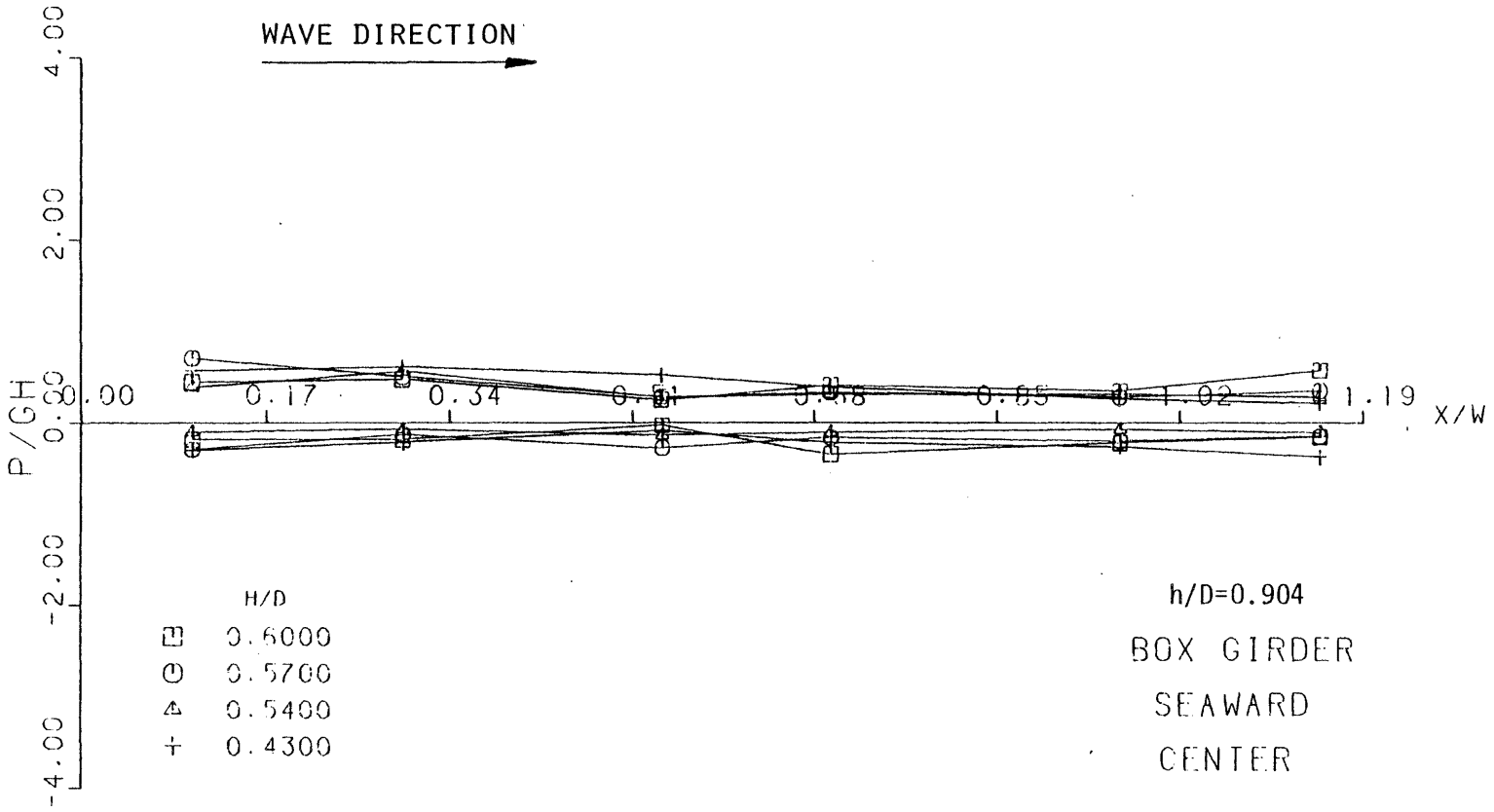
WAVE DIRECTION
4.00
2.00
0.00
-2.00
-4.00
P/GH
0.00
0.17
0.34
0.85
1.02
1.19
X/W
H/D
0.6000
0.5700
0.5400
0.4300
h/D=0.904
BOX GIRDER
SEAWARD
CENTER

Figure C.1

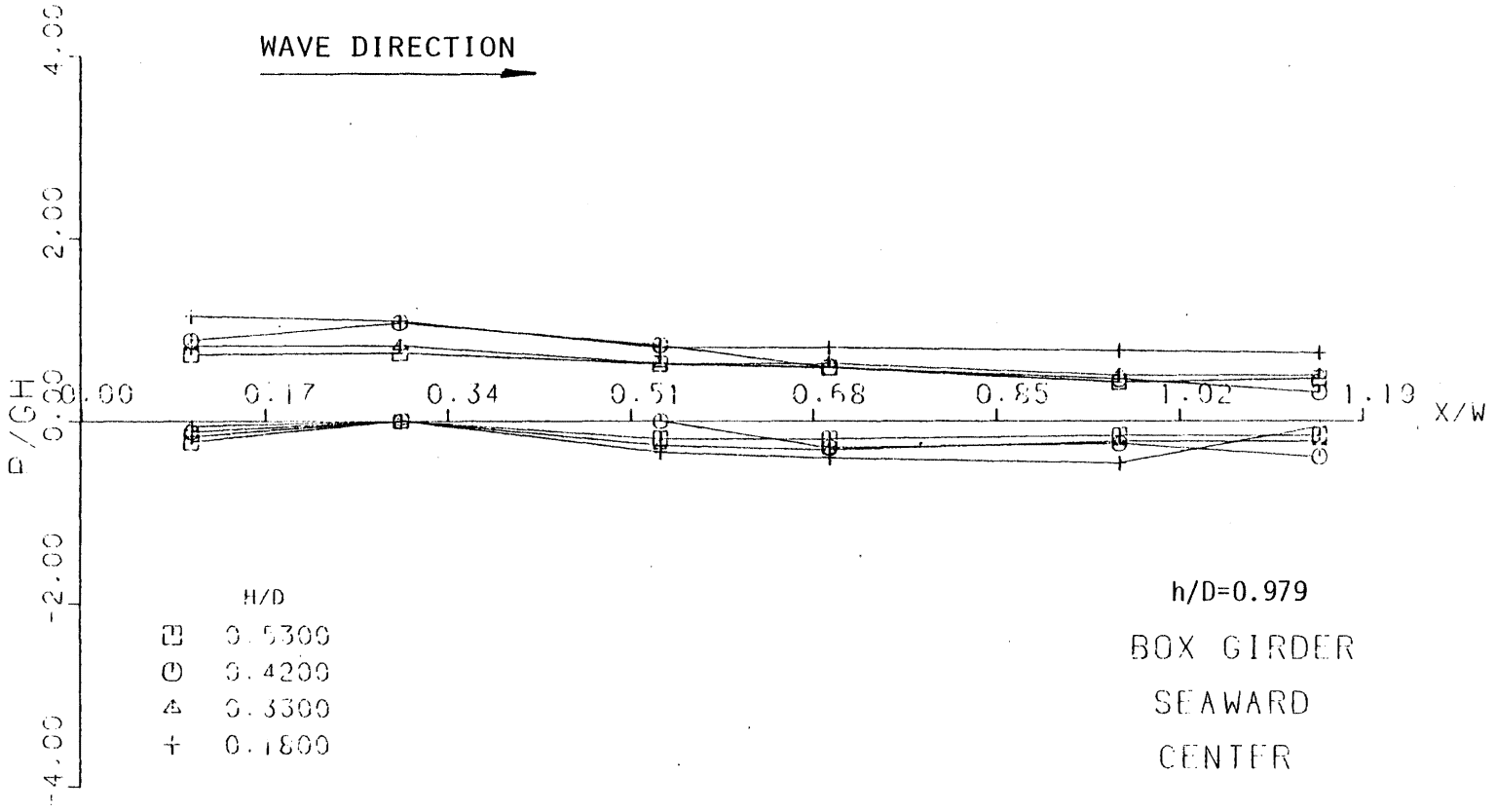

Figure C.2

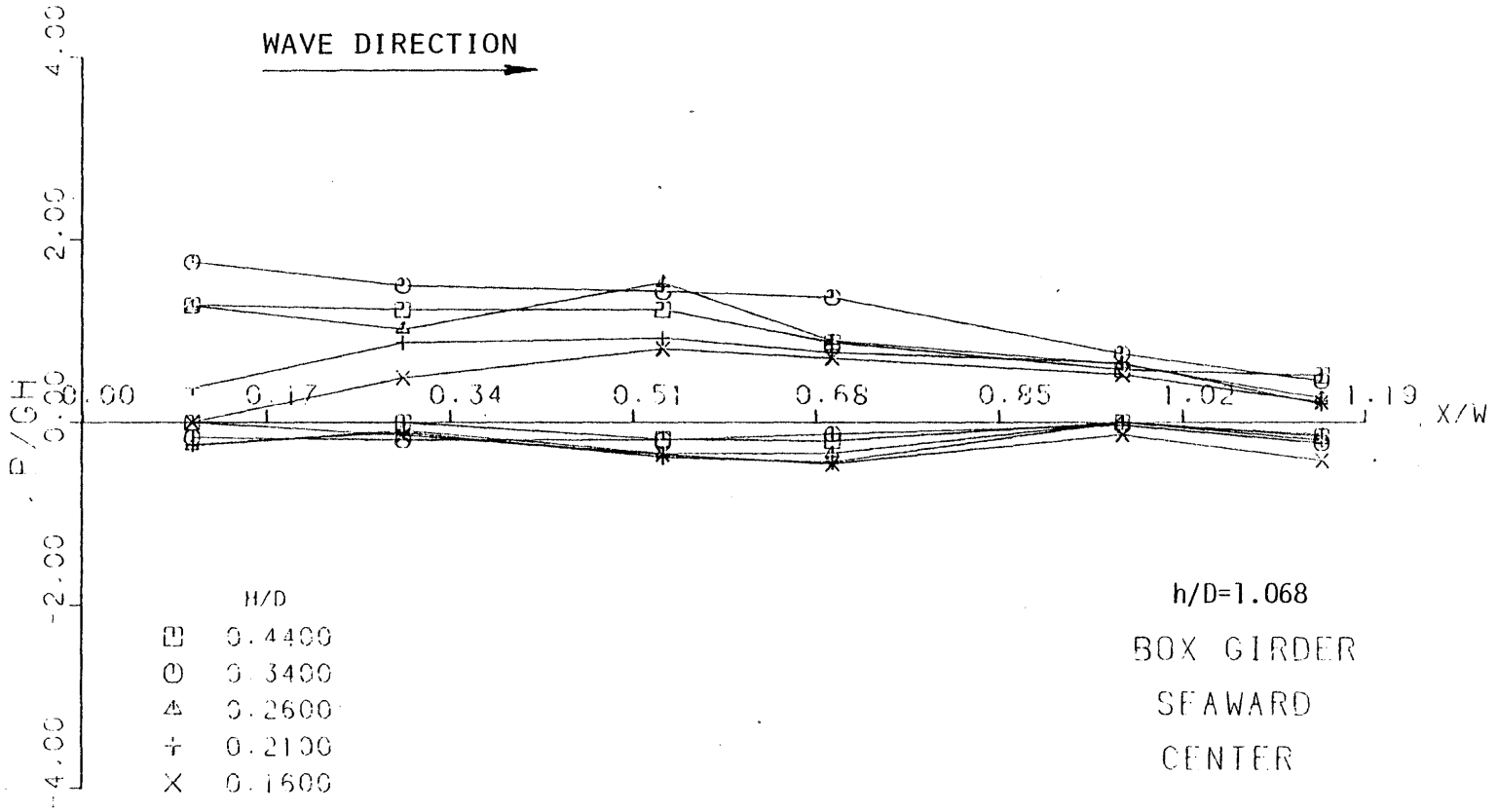
WAVE DIRECTION
4.00
2.00
0.00
-2.00
-4.00
D/SH
0.00
0.17
0.34
0.51
0.68
0.85
1.02
1.19
X/W
H/D
0.4400
0.3400
0.2600
0.2100
0.1600
h/D=1.068
BOX GIRDER
SEAWARD
CENTER

Figure C.3

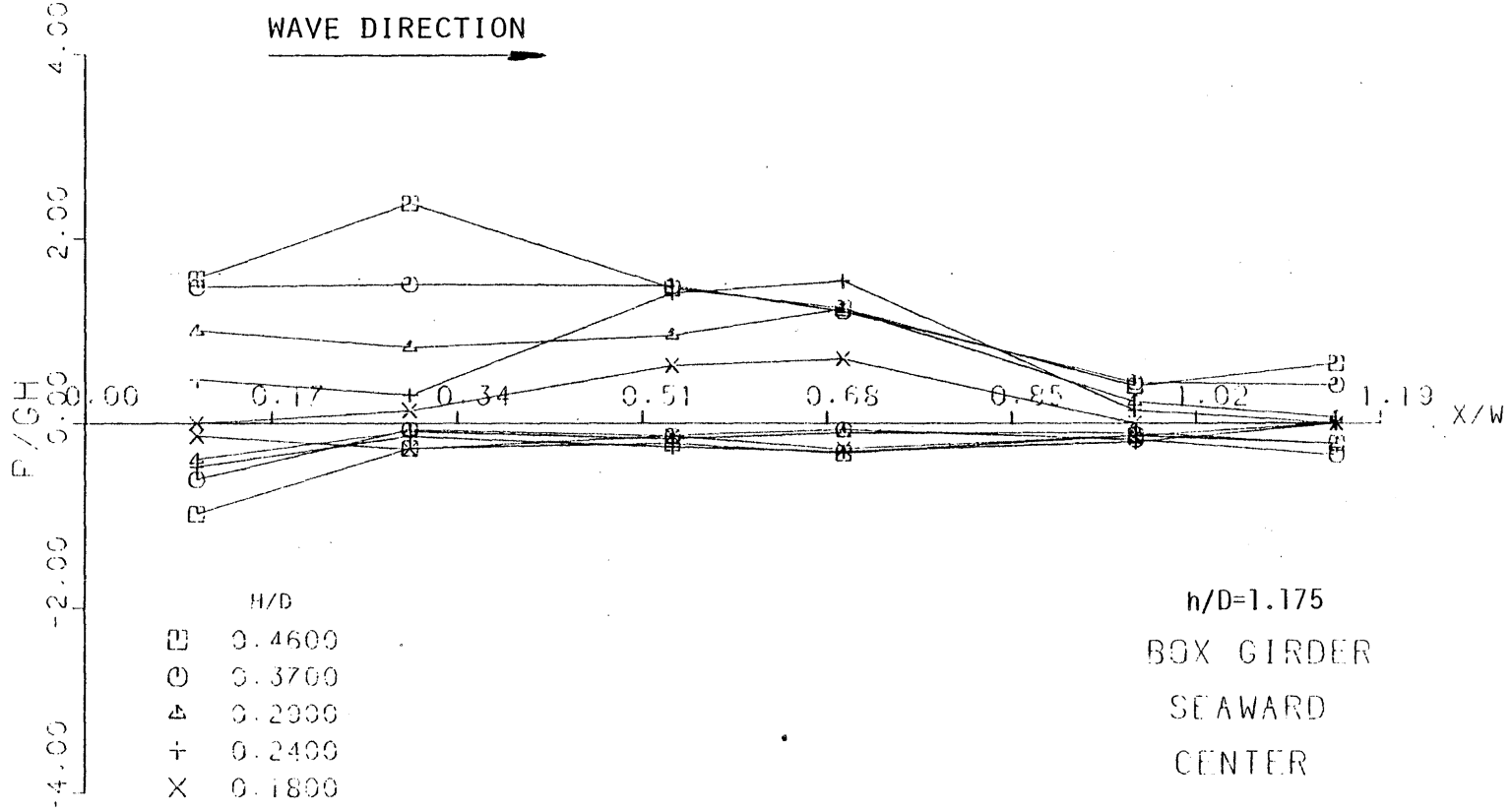

Figure C.4

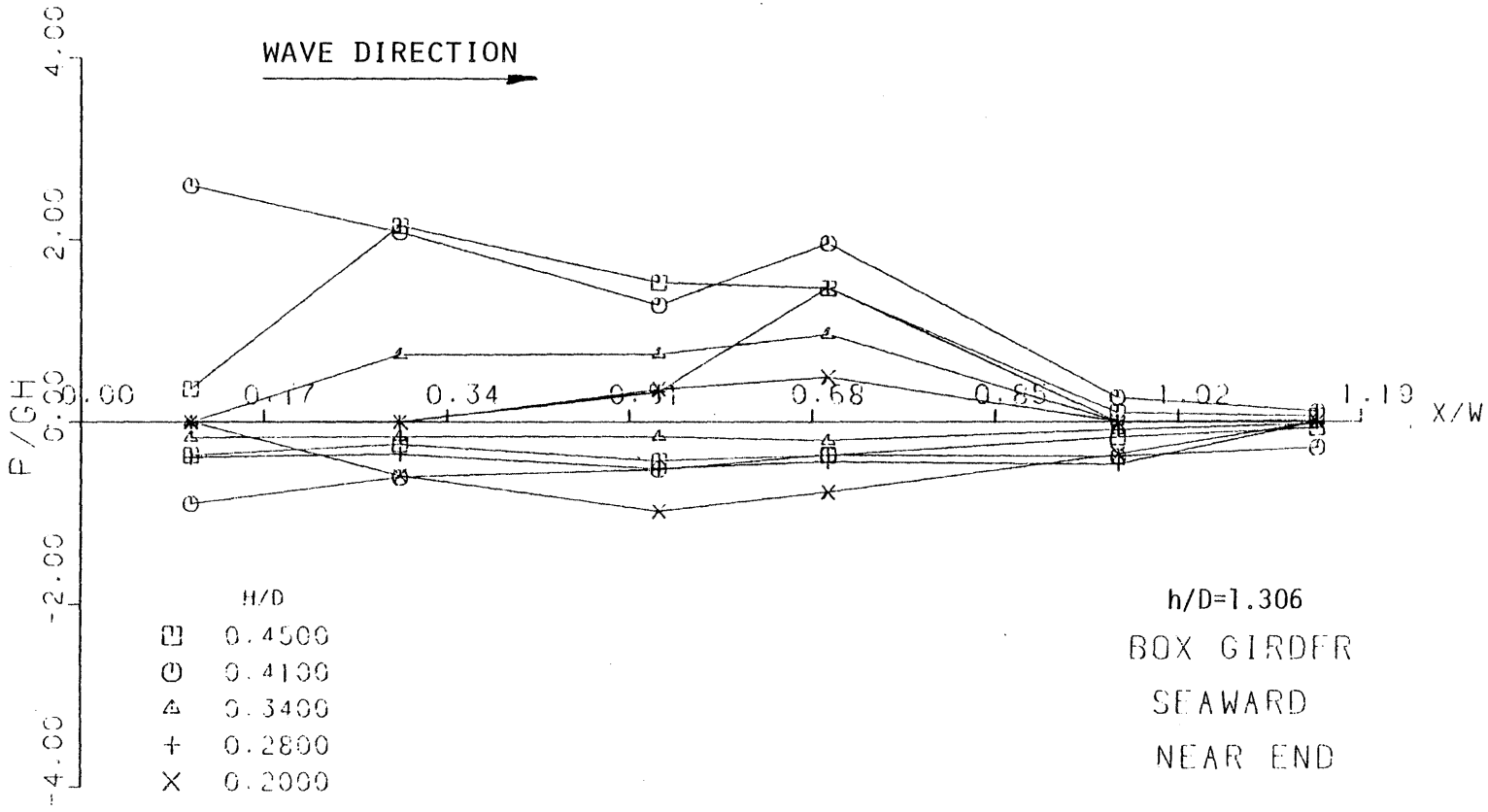
WAVE DIRECTION
4.00
2.00
0.00
-2.00
-4.00
P/GH
0.00
0.17
0.34
0.51
0.68
0.85
1.02
1.19
X/W
H/D
0.4500
0.4100
0.3400
0.2800
0.2000
h/D=1.306
BOX GIRDER
SEAWARD
NEAR END

Figure C.5

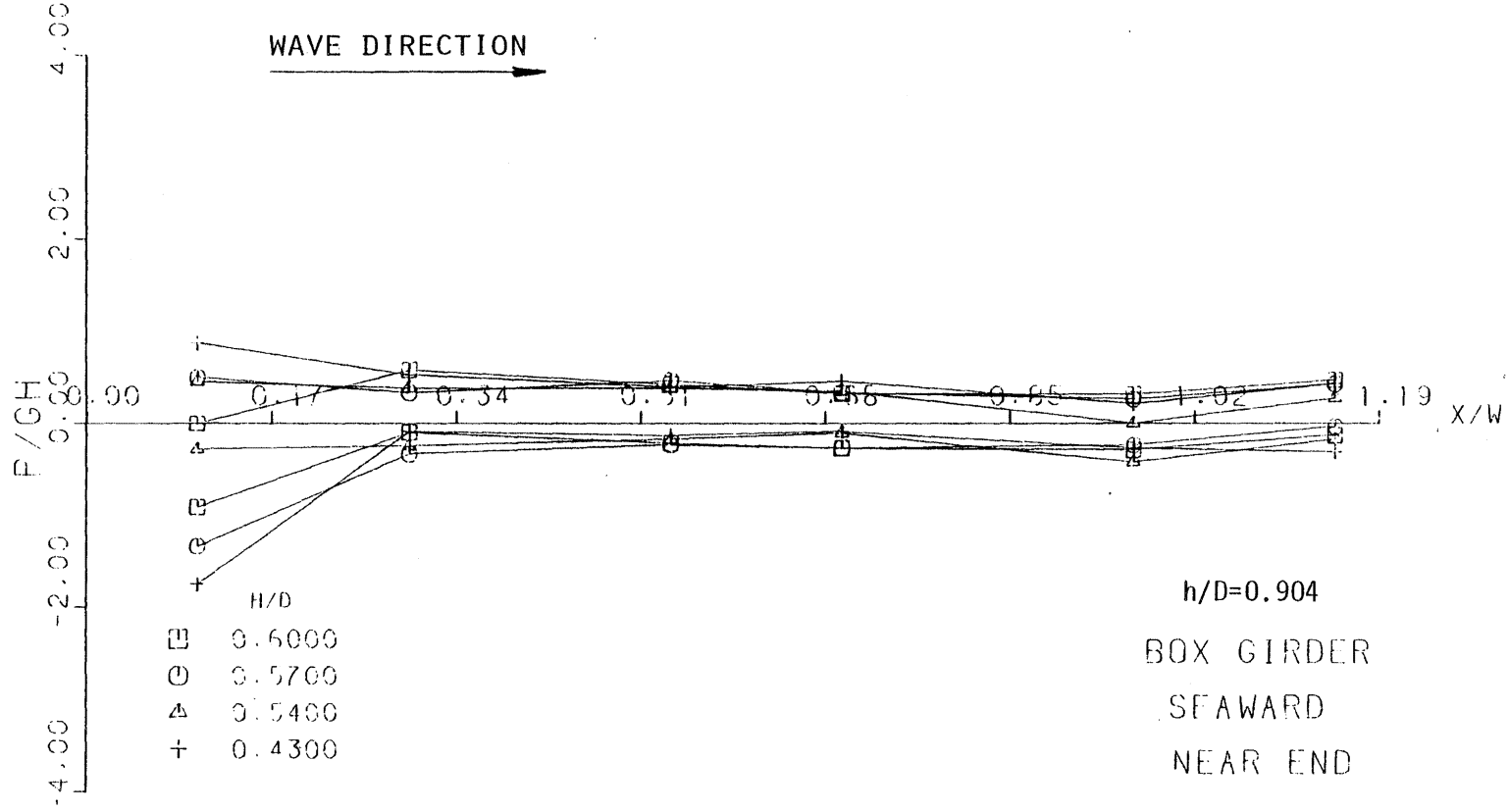

Figure C.6

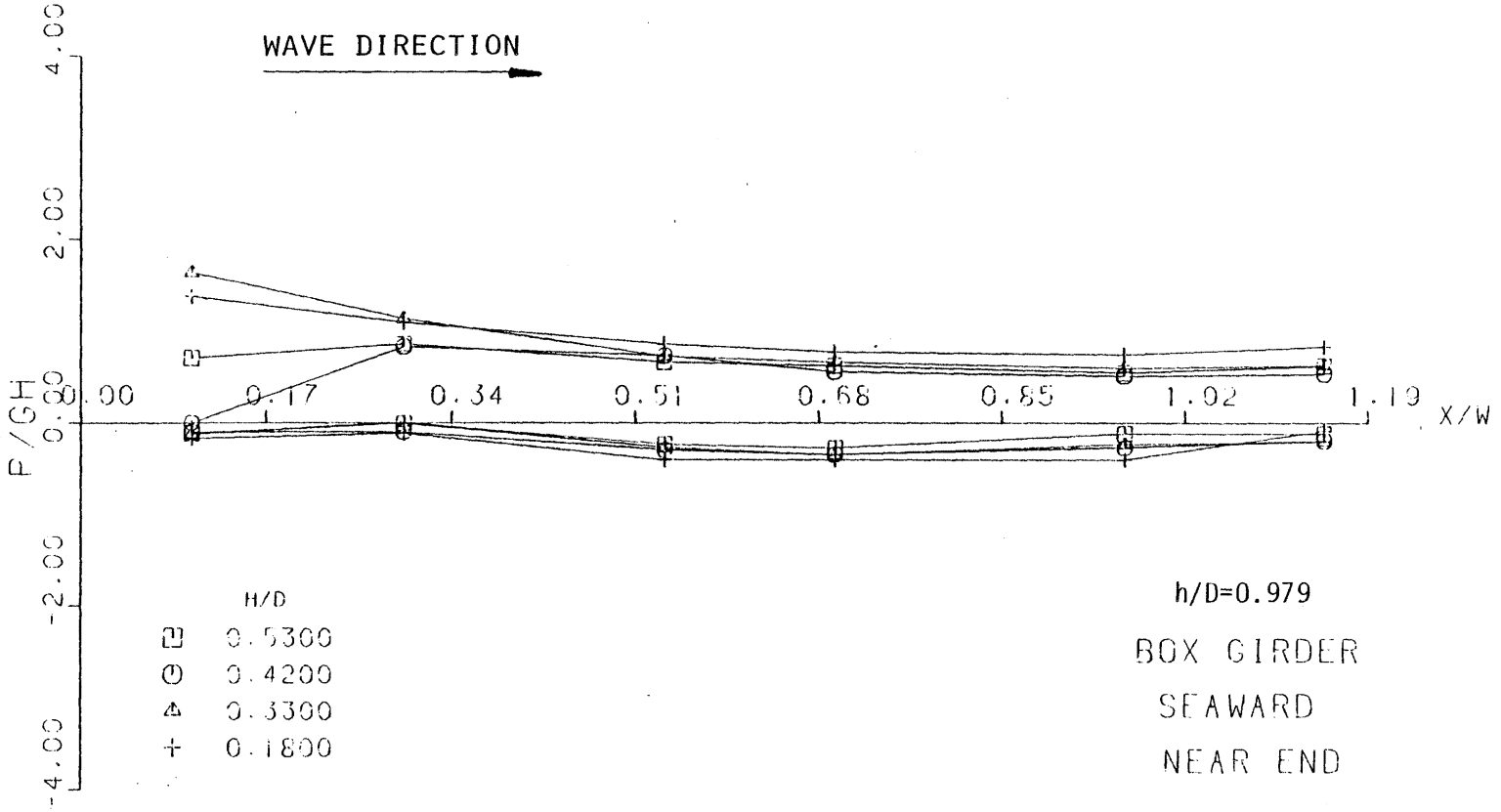
WAVE DIRECTION
4.00
2.00
0.00
-2.00
-4.00
F/GH
0.00
0.17
0.34
0.51
0.68
0.85
1.02
1.19
X/W
H/D
0.5300
0.4200
0.3300
0.1800
h/D=0.979
BOX GIRDER
SEAWARD
NEAR END

Figure C.7

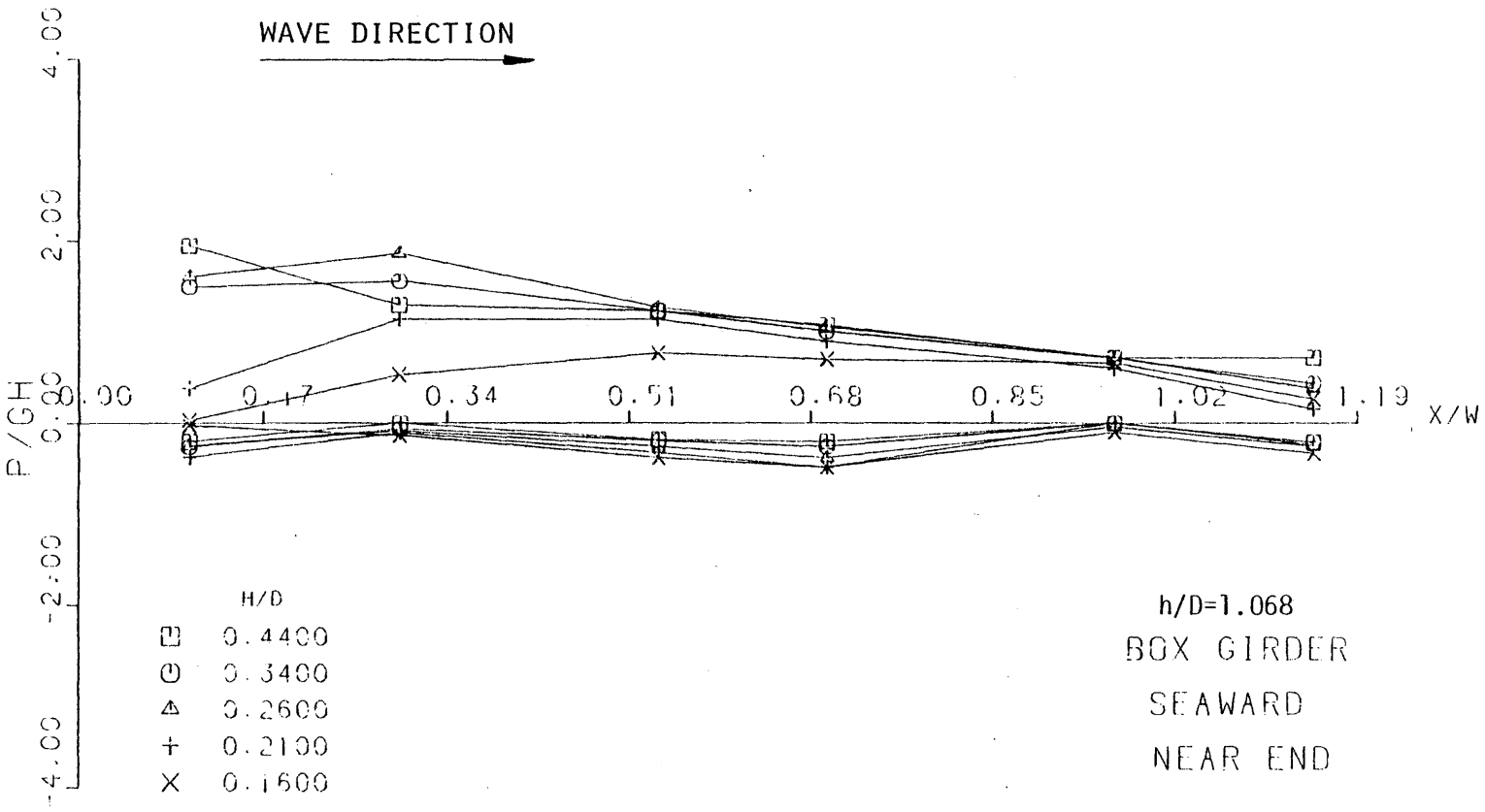
WAVE DIRECTION
4.00
2.00
0.00
-2.00
-4.00
P/GH
0.00
0.17
0.34
0.51
0.68
0.85
1.02
1.19
X/W
H/D
0.4400
0.3400
0.2600
0.2100
0.1600
h/D=1.068
BOX GIRDER
SEAWARD
NEAR END

Figure C.8

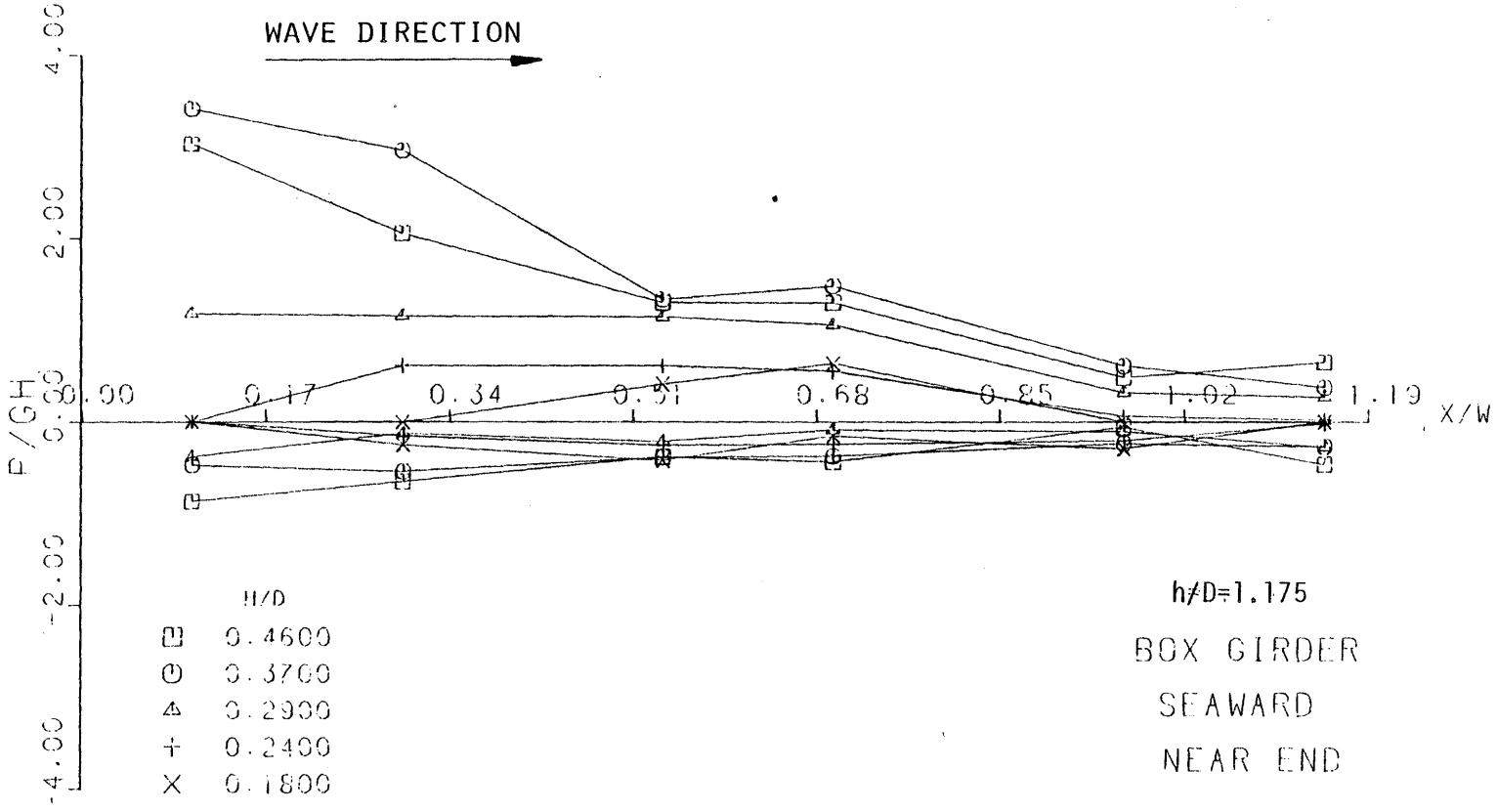

Figure C.9

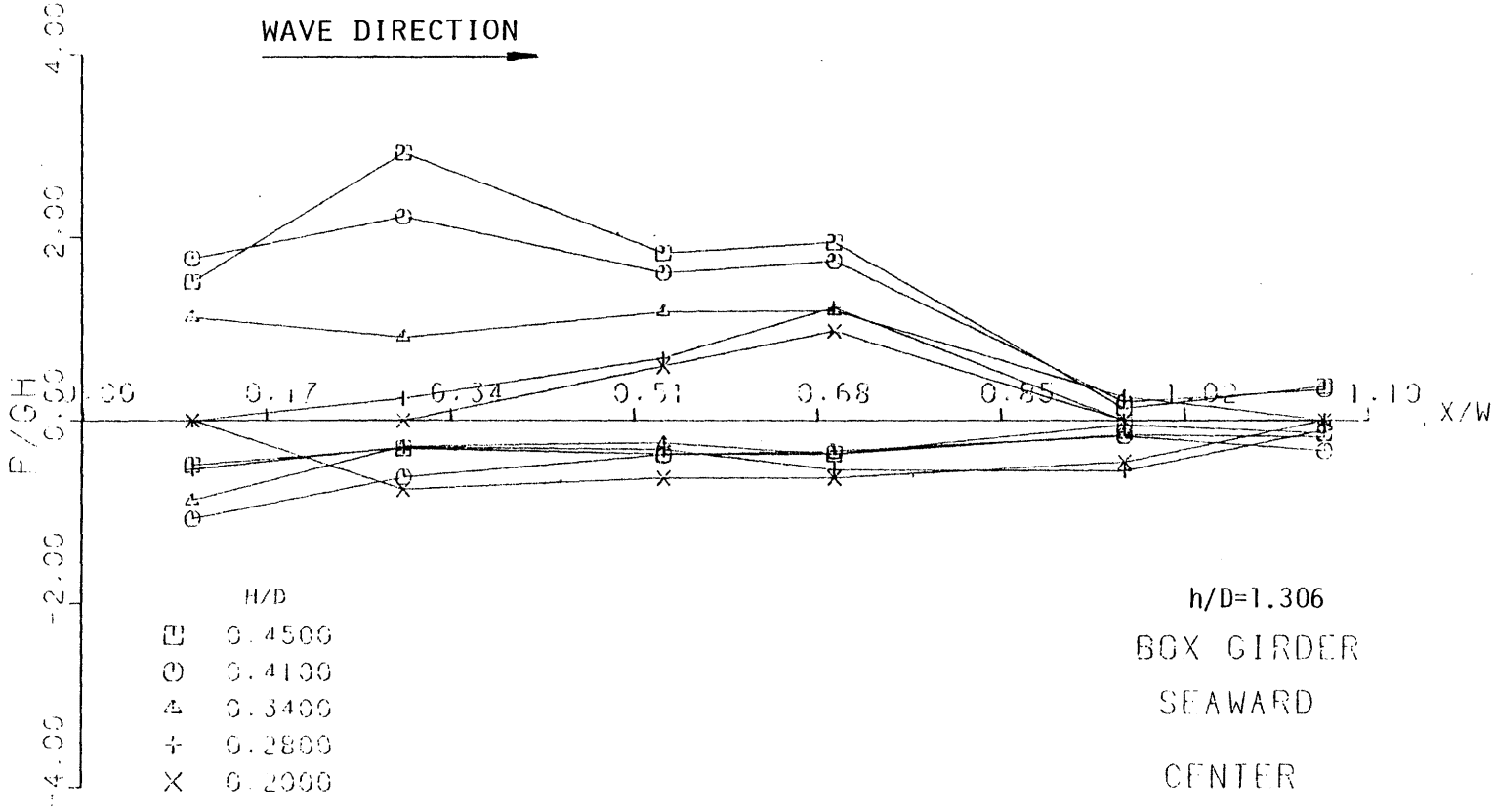
WAVE DIRECTION
4.00
2.00
0.00
-2.00
-4.00
η/GH
0.00
0.17
0.34
0.51
0.68
0.85
1.02
1.19
X/W
H/D
0.4500
0.4100
0.3400
0.2800
0.2000
h/D=1.306
BOX GIRDER
SEAWARD
CENTER

Figure C.10

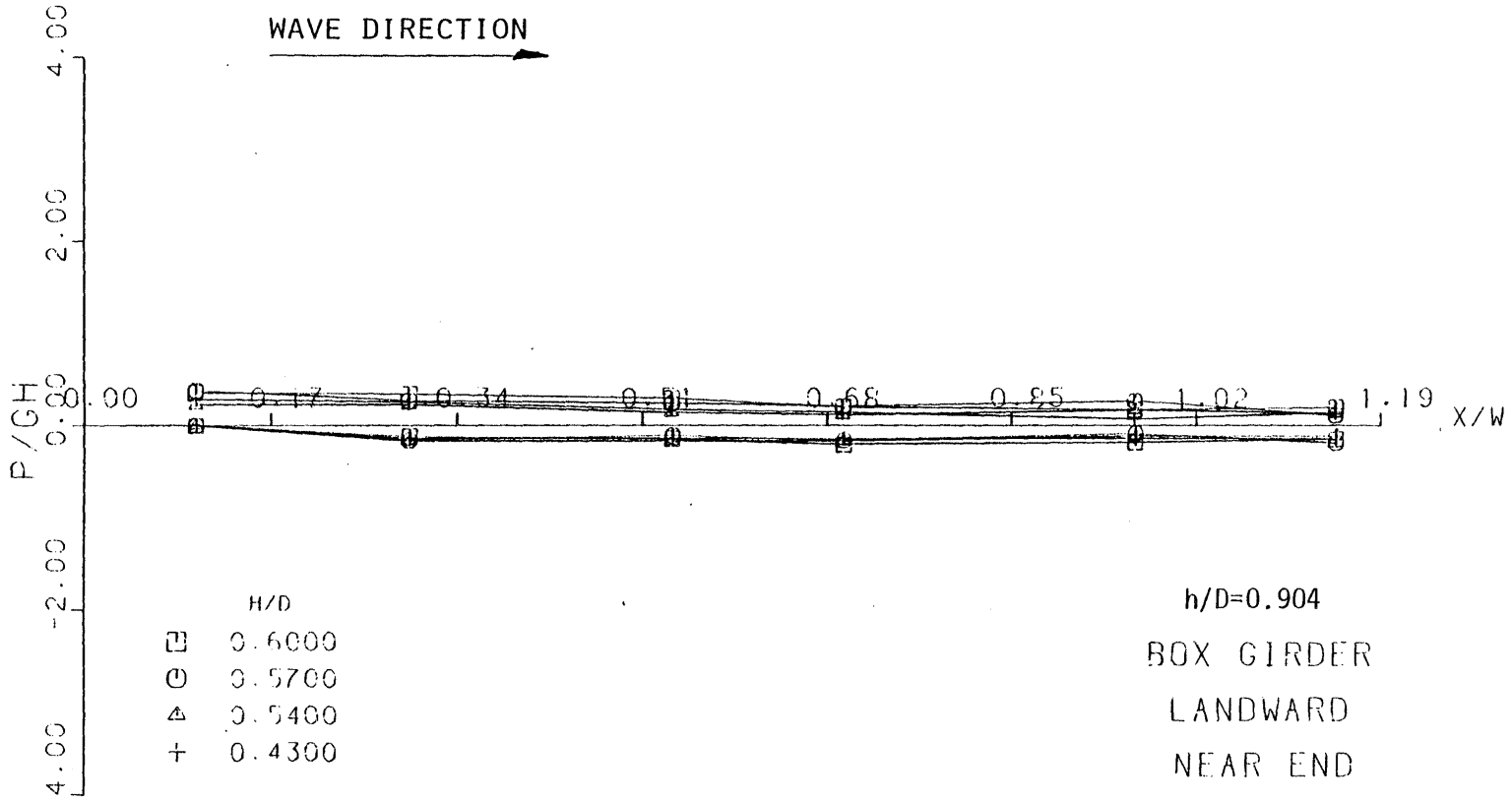
WAVE DIRECTION
4.00
2.00
0.00
-2.00
-4.00
P/GH
0.00
0.17
0.34
0.51
0.68
0.85
1.02
1.19
X/W
H/D
0.6000
0.5700
0.5400
0.4300
h/D=0.904
BOX GIRDER
LANDWARD
NEAR END

Figure C.11

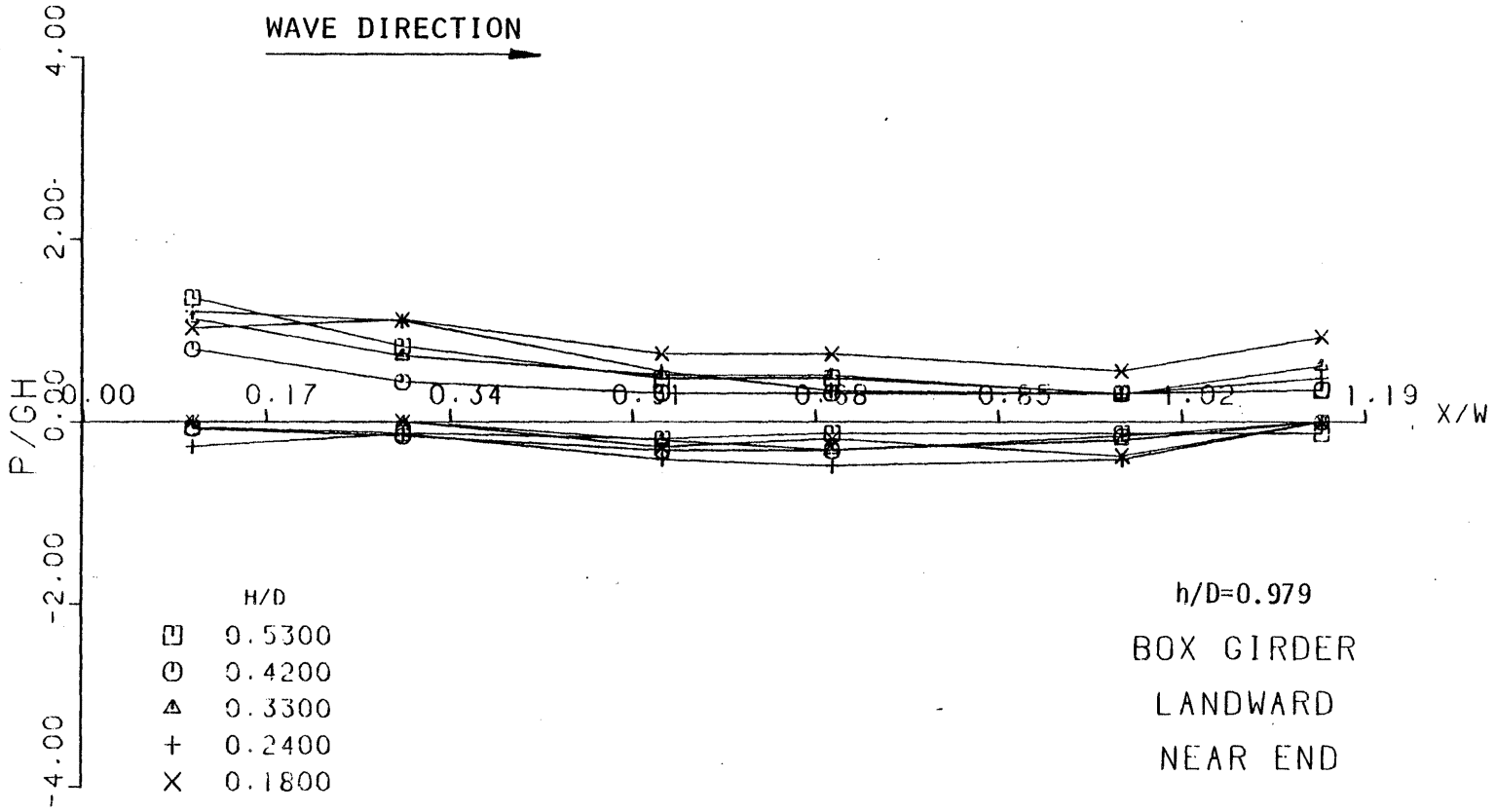
WAVE DIRECTION
4.00
2.00
0.00
-2.00
-4.00
P/GH
0.00
0.17
0.34
0.51
0.68
0.85
1.02
1.19
X/W
H/D
0.5300
0.4200
0.3300
0.2400
0.1800
h/D=0.979
BOX GIRDER
LANDWARD
NEAR END

Figure C.12

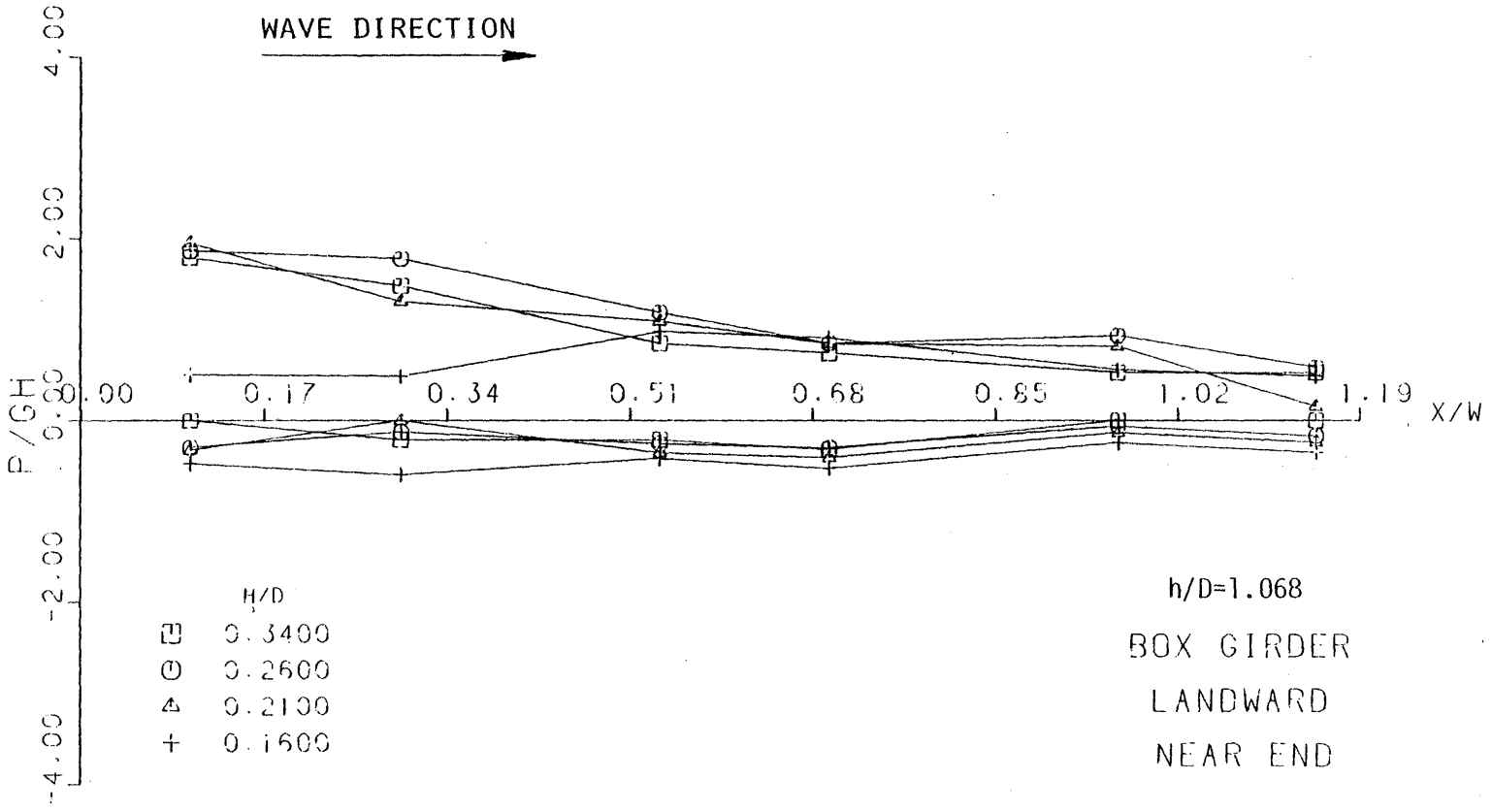
WAVE DIRECTION
4.00
2.00
0.00
-2.00
-4.00
P/GH
0.00
0.17
0.34
0.51
0.68
0.85
1.02
1.19
X/W
H/D
0.3400
0.2600
0.2100
0.1600
h/D=1.068
BOX GIRDER
LANDWARD
NEAR END

Figure C.13

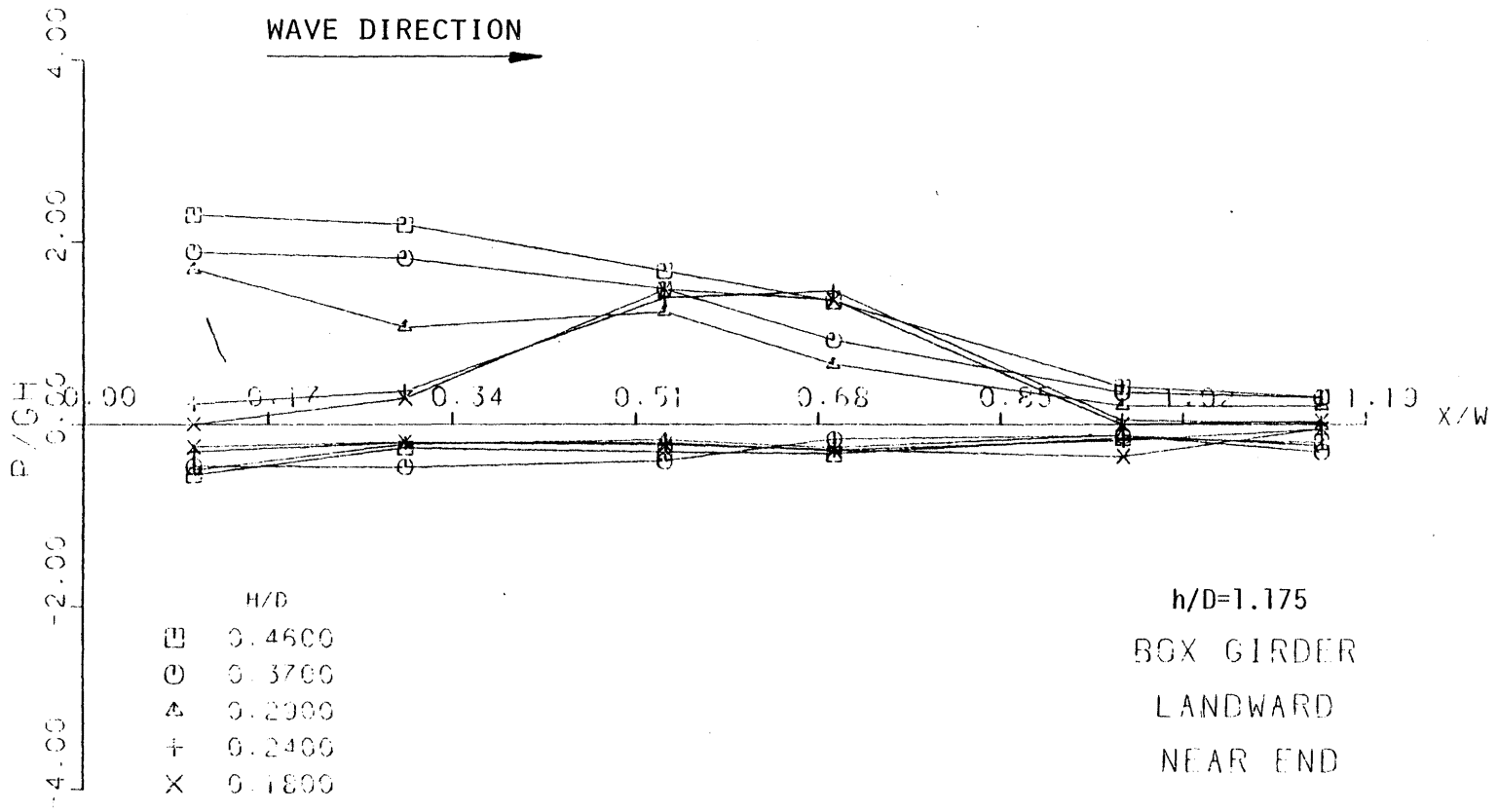

Figure C.14

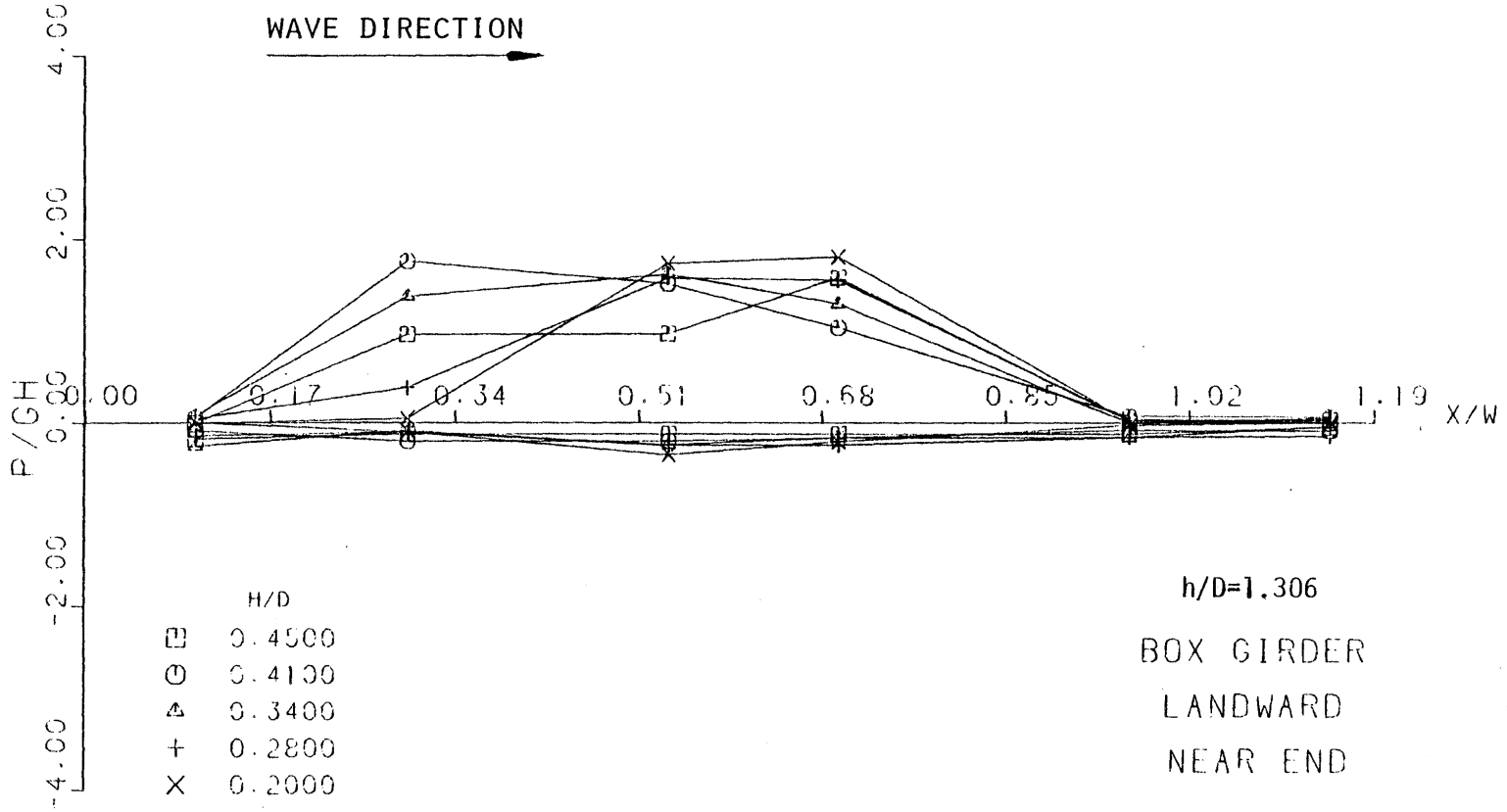
WAVE DIRECTION
4.00
2.00
0.00
-2.00
-4.00
P/GH
0.00
0.17
0.34
0.51
0.68
0.85
1.02
1.19
X/W
H/D
0.4500
0.4100
0.3400
0.2800
0.2000
h/D=1.306
BOX GIRDER
LANDWARD
NEAR END

Figure C.15

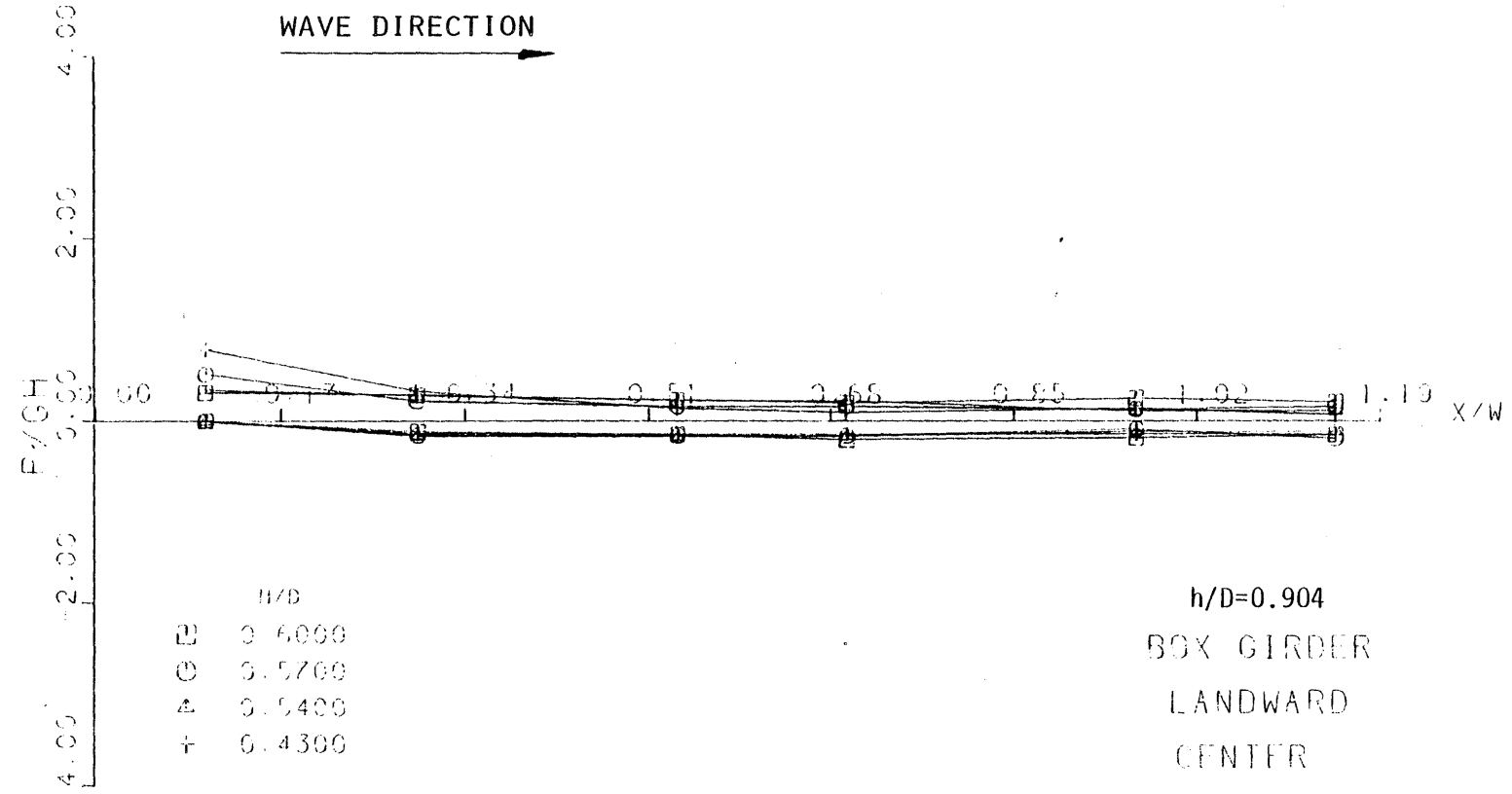

Figure C.16

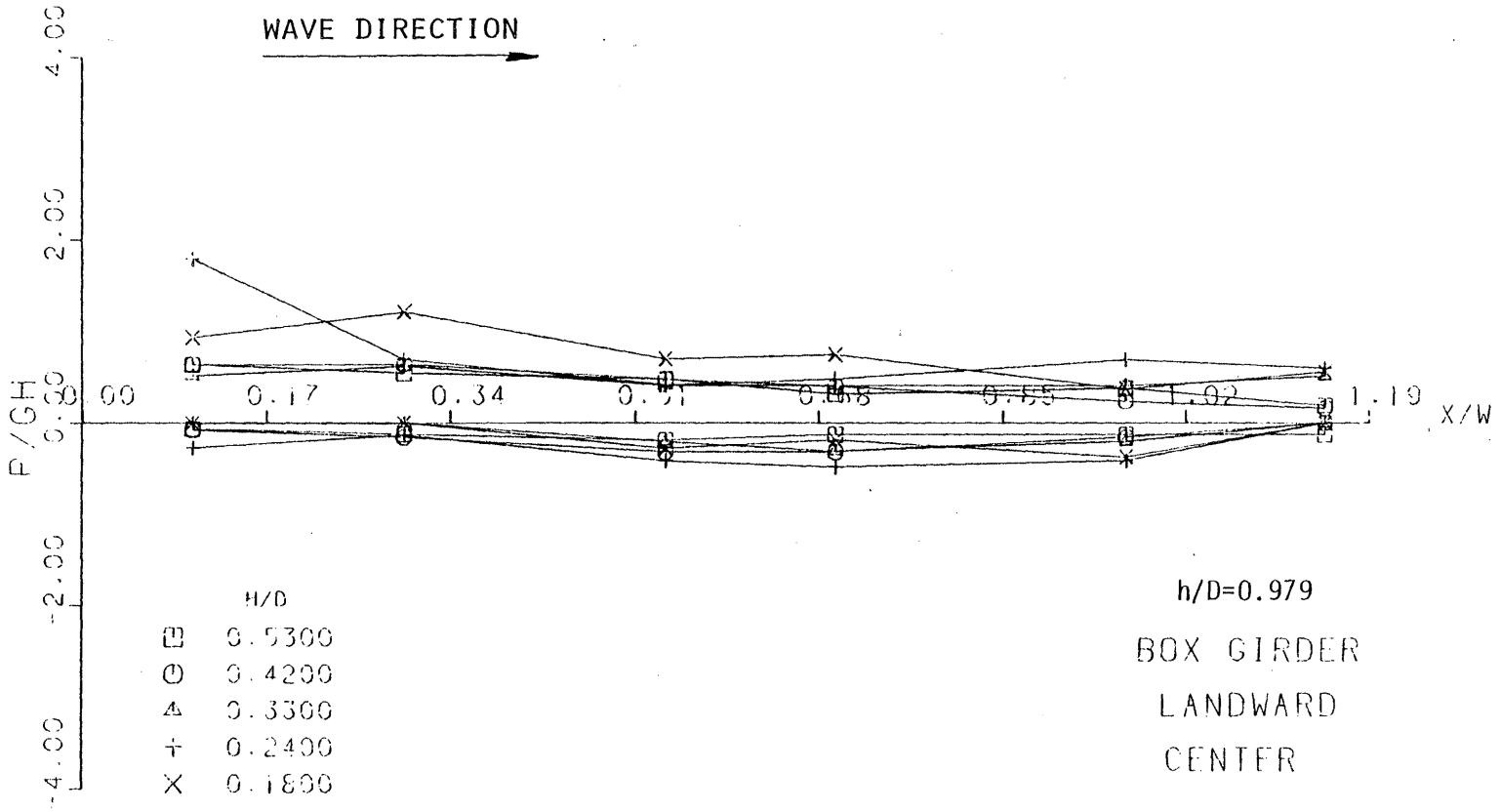
WAVE DIRECTION
4.00
2.00
0.00
-2.00
-4.00
P/GH
0.00
0.17
0.34
0.51
0.68
0.85
1.02
1.19
X/W
H/D
0.5300
0.4200
0.3300
0.2400
0.1800
h/D=0.979
BOX GIRDER
LANDWARD
CENTER

Figure C.17

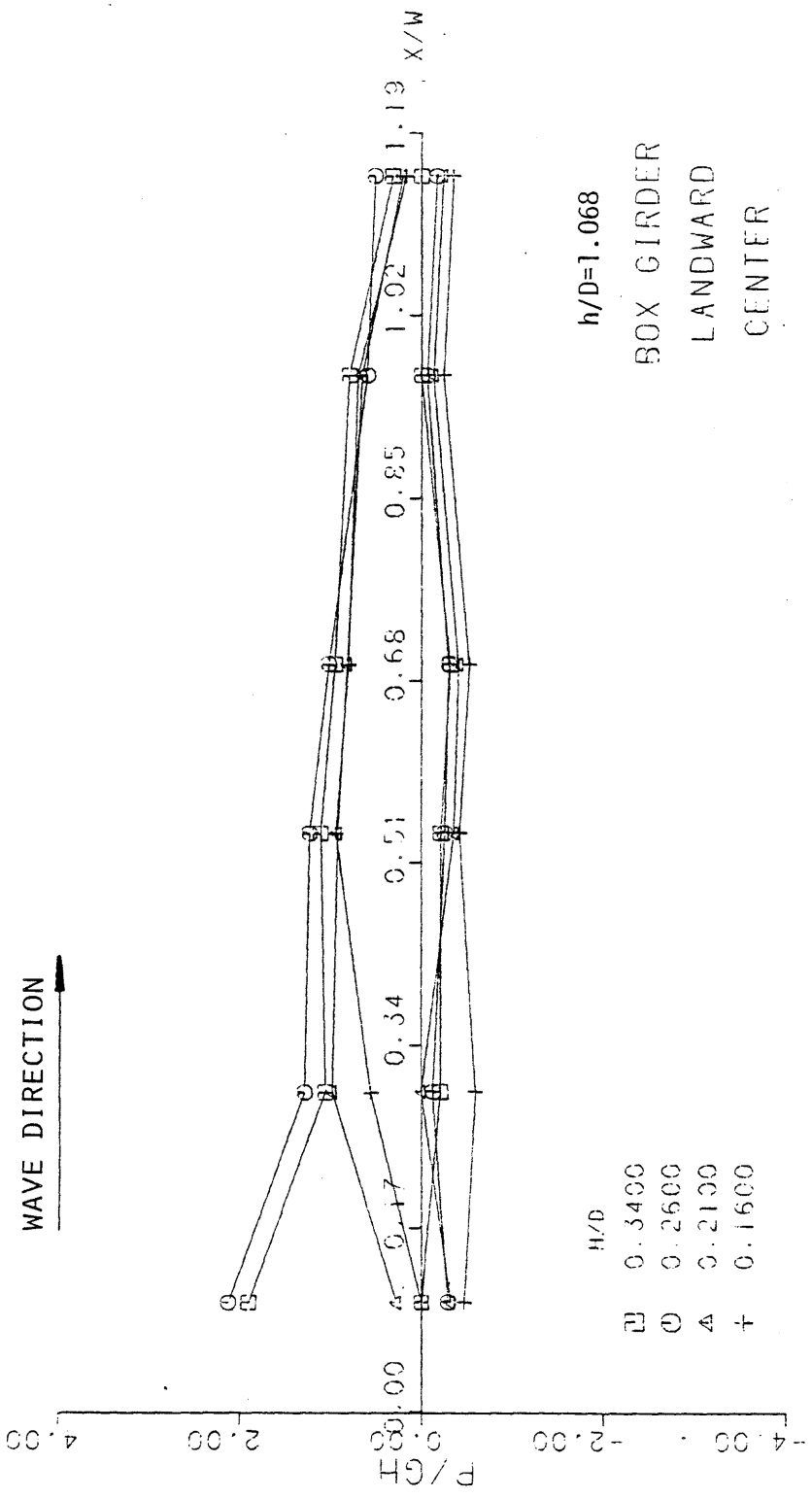
WAVE DIRECTION
h/D=1.068
BOX GIRDER
LANDWARD
CENTER
X/W
0.00
0.17
0.34
0.51
0.68
0.85
1.02
1.19
P/GH
4.00
2.00
0.00
-2.00
-4.00
H/D
0.3400
0.2600
0.2100
0.1600

Figure C.18

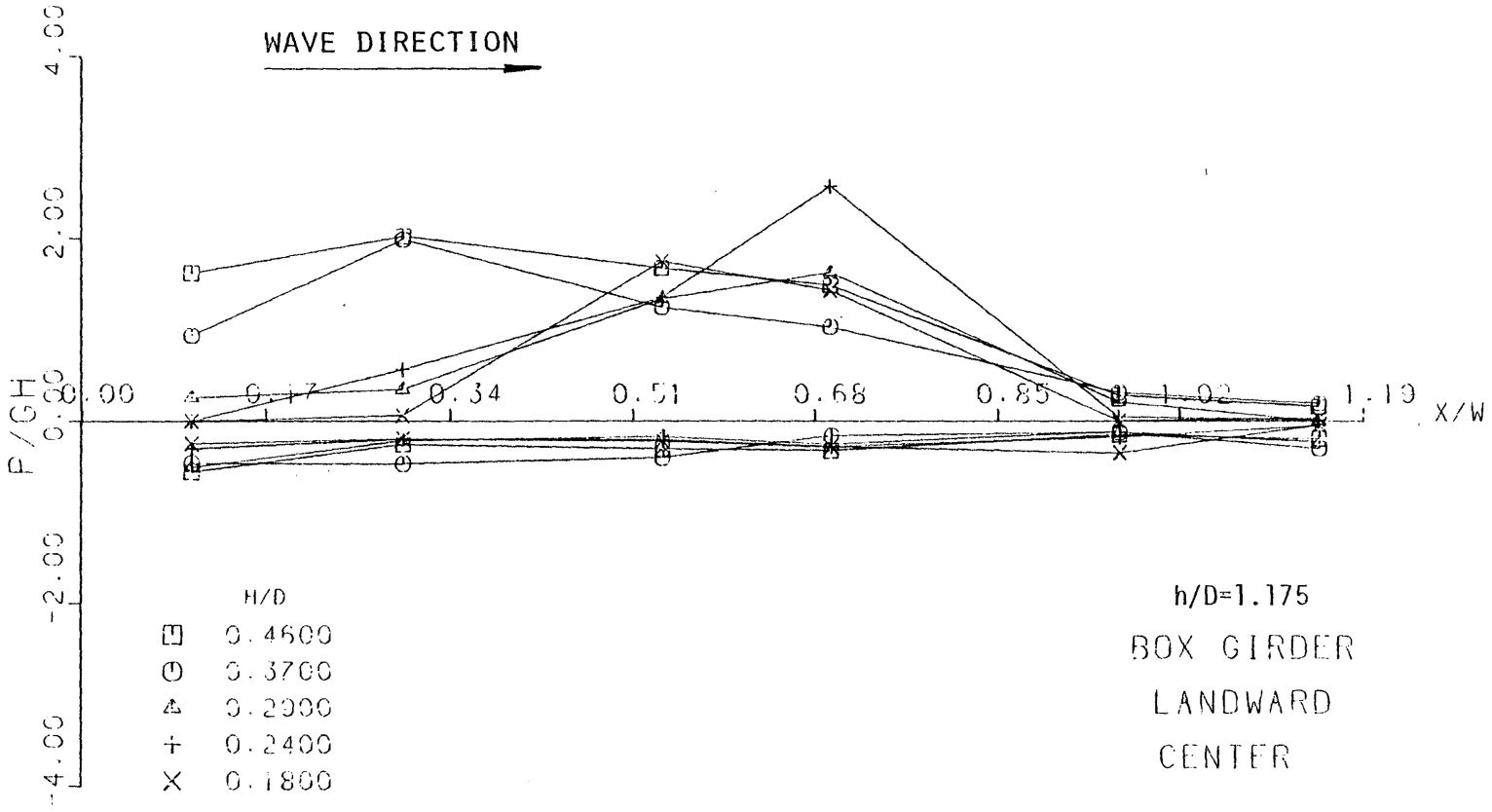

Figure C.19

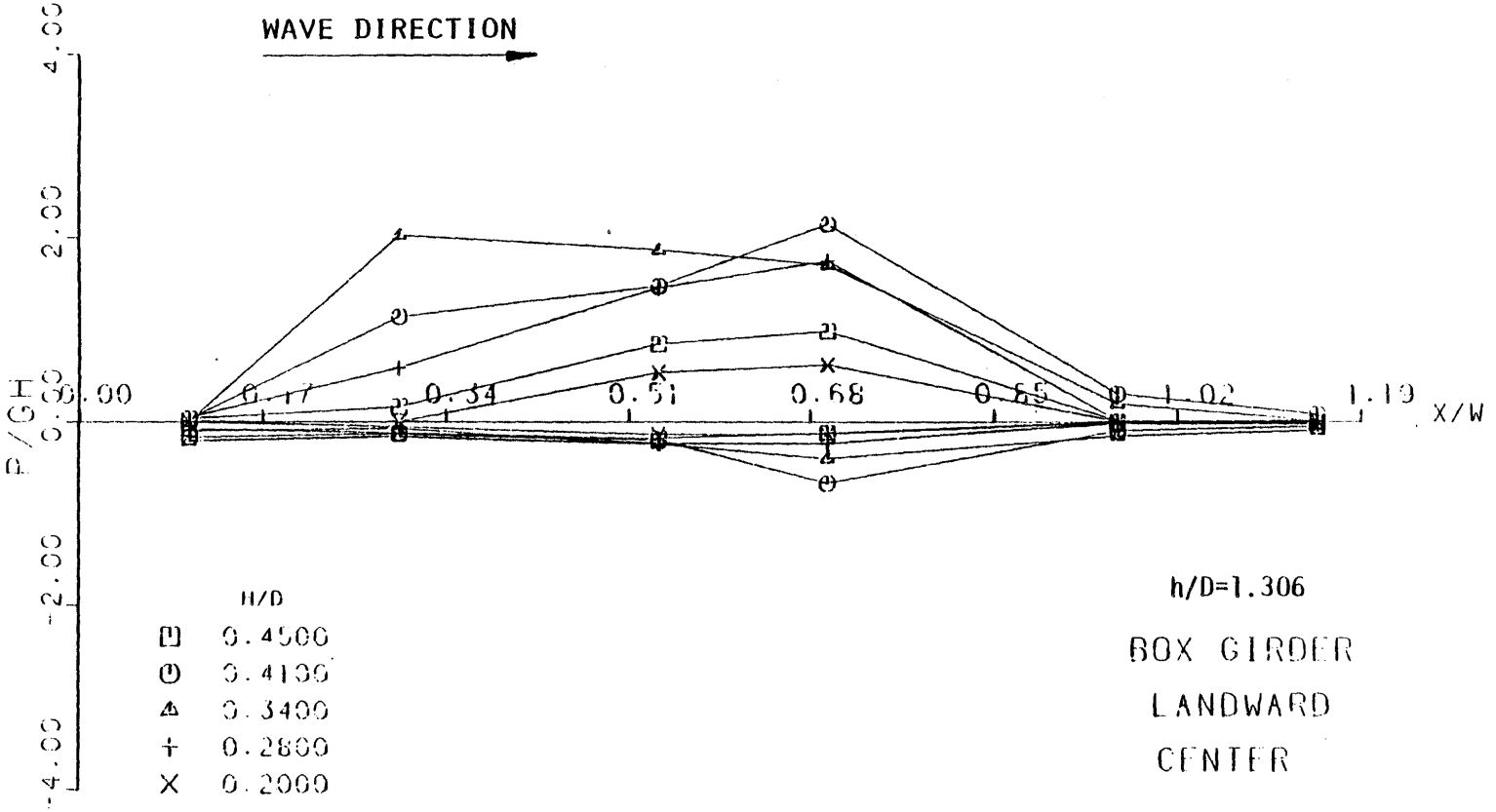
WAVE DIRECTION
4.00
2.00
0.00
-2.00
-4.00
η/GH
0.00
0.17
0.34
0.51
0.68
0.85
1.02
1.19
X/W
H/D
0.4500
0.4100
0.3400
0.2800
0.2000
h/D=1.306
BOX GIRDER
LANDWARD
CENTER

Figure C.20